5 Lock Wall Simulation

In Chapter 4, it was shown that the extended hyperbolic model accurately predicts the interface response for a variety of experimental stress paths applied in the laboratory. It is desirable, however, to evaluate the accuracy and applicability of this new model for SSI analyses of lock walls. There are little data on lock wall response during construction and operation of locks that can be used to perform such an evaluation. The IRW at Virginia Tech provides a unique opportunity to model key aspects of lock wall construction and operation within a controlled experimental environment.

The IRW was originally developed to study the earth pressures induced by compaction of backfill. Factors such as type of backfill, compaction procedure, and lateral movements of the wall were analyzed by Sehn (1990) and Filz (1992) using the IRW. As result of their work, methods were developed for estimation of compaction-induced earth pressures against retaining walls (Duncan et al. 1991; Filz and Duncan 1997; Filz, Duncan, and Ebeling 1997).

For this investigation, a test was performed in the IRW that modeled placement and compaction of the backfill, application and removal of surcharge, and movements of the water table behind a lock wall. Light Castle Sand was used as backfill material for the test. Finite element analyses of all the stages of the test were performed using the updated version of SOILSTRUCT-ALPHA, which contains the formulation of the extended hyperbolic model for interfaces. Analyses of the backfill and surcharge stages served to calibrate the backfill properties for use in analyses of the inundation stage. The test results indicate that the extended hyperbolic model provides accurate approximations of the response of the wall-backfill interface for the type of loading induced during the test.

This chapter describes the experimental procedures, results of the IRW test, and analyses of the IRW test. The chapter is divided into the following sections:

1. The IRW facility.

2. Testing procedures.

3. Test results.

4. Discussion of test results.

5. Finite element analysis procedures.

6. Calibration analyses.

7. Analysis of backfill inundation.

8. Summary and conclusions.

The first section describes the characteristics of the IRW and the modifications that were necessary to accommodate simulation of a lock wall. In subsequent sections, the testing procedures and results are described in detail. Some observations are presented regarding the backfill response to external loading and compaction that are relevant for the finite element analyses of the IRW. Details of the analyses performed using SOILSTRUCT-ALPHA are also presented. Finally, the accuracy of the extended hyperbolic model is evaluated based on comparisons of the results of the analyses and the test data.

5.1 The Instrumented Retaining Wall (IRW) Facility

A complete description of the components of the IRW was presented by Sehn (1990). This section summarizes the features of the IRW that are relevant for this investigation.

5.1.1 Components of the IRW

Figure 5-1 is a general view of the IRW. It is composed of a backfill area, the instrumented wall, and a reinforced concrete U-frame structure that supports the wall and encloses the backfill area. The IRW is located inside a building, isolated from the direct action of the elements. An overhead crane facilitates movement of heavy equipment and materials. The floor of the backfill area is approximately 0.90 m below the floor level of the surrounding areas in the building. The top of the instrumented wall is approximately 1.20 m above the floor level of the building. The backfill area is 1.83 m wide by 3.05 m long. A 1.83-m-wide ramp leading into the area provides access for the equipment necessary for placement and compaction of the backfill.

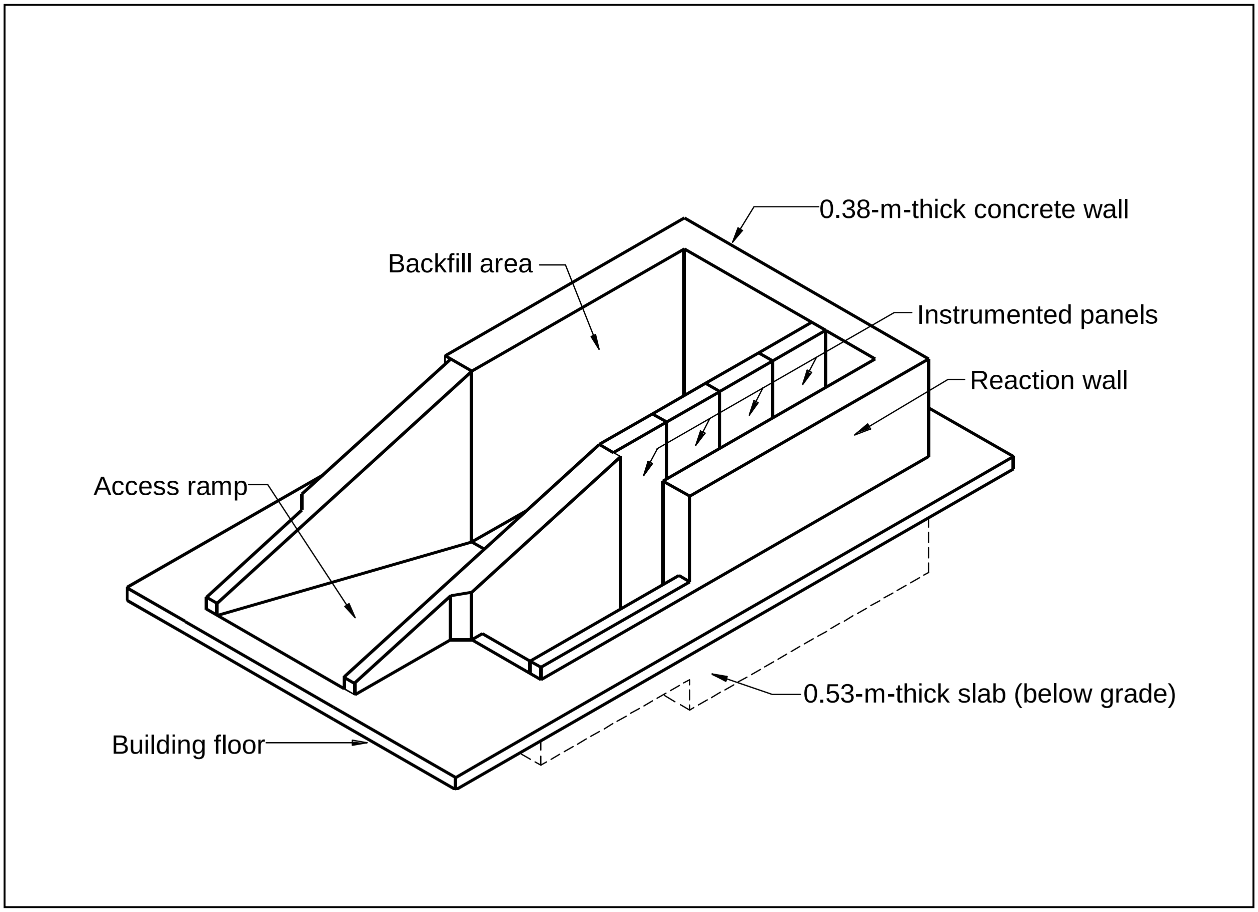

Figure 5-1. The IRW test facility (after Sehn 1990)

A cross section of the IRW is shown in Figure 5-2. The instrumented wall is composed of four 0.73-m-wide by 2.13-m-high concrete panels. Each of the panels is supported vertically by two cantilever-type load cells (Sehn 1990), which consist of a 0.1-m-long cantilever beam bolted to a support bracket at the bottom of the panel. On the free end of the beam, a roller bearing wheel allows movement on a hardened steel pad attached to the concrete floor. Each of the panels is supported horizontally by three horizontal load cells. Each of the load cells consists of a steel bar, supported on both ends by spherical bearings to minimize bending moments. The forces on the vertical and horizontal load cells are measured by strain gauges bonded to their surface at appropriate locations.

The horizontal loads from the panels are transmitted by the load cells to a steel frame behind the panels. The frame is supported vertically by bearings that allow horizontal movements. Four screw jacks allow the application of horizontal displacements to the instrumented wall. This feature of the IRW was not used in the lock wall simulation. The concrete panels were kept in place throughout the test.

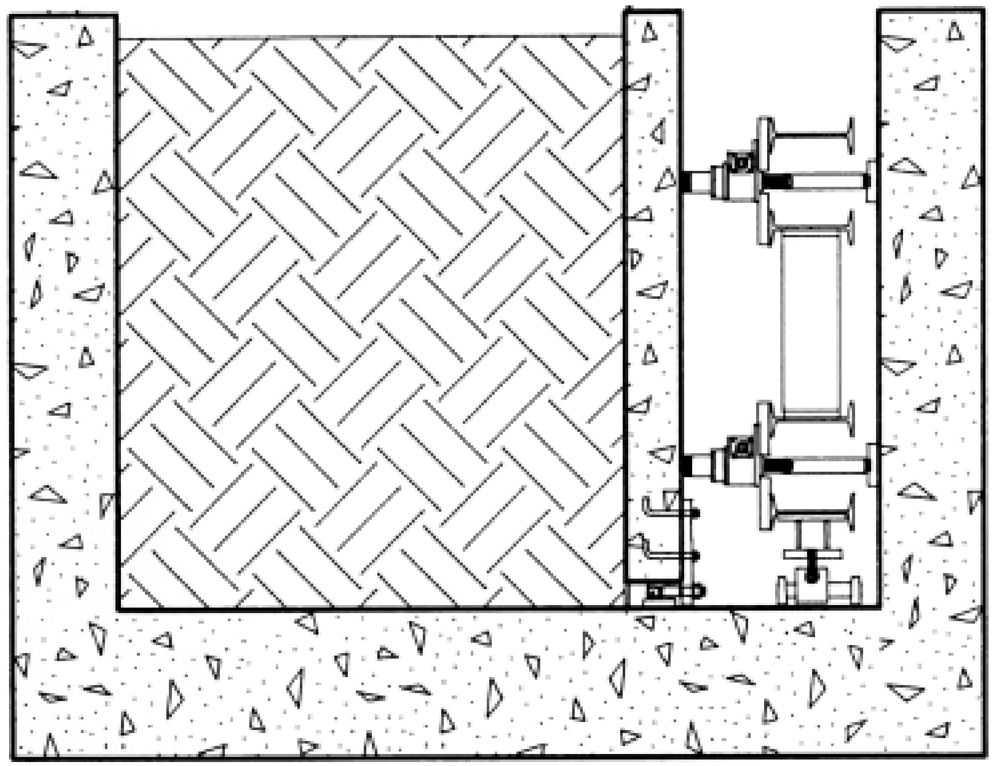

Figure 5-2. Cross-section of the IRW

The displacements of each of the panels during testing are monitored by two LVDTs located at the top and bottom of the panel. The LVDTs are attached to a fixed reference beam located behind the panels.

As illustrated in Figure 5-3, the two central panels of the instrumented wall contain a variety of pressure cells for local measurements of earth pressures. Sehn (1990) present a detailed description of the type of pressure cells embedded in the panels. For this investigation, pressures were measured using only the Gloetzl cells. The Gloetzl cells are mounted flush with the exposed wall surface. The surface of each of the cells is coated with a cement grout that resembles the surface texture of the wall. It was found that the Gloetzl cells did not provide accurate data, especially during inundation of the backfill. Filz (1992) recognized that these pressure cells may be especially sensitive to moisture migration in the surrounding mass of concrete. Nevertheless, pressure data collected during

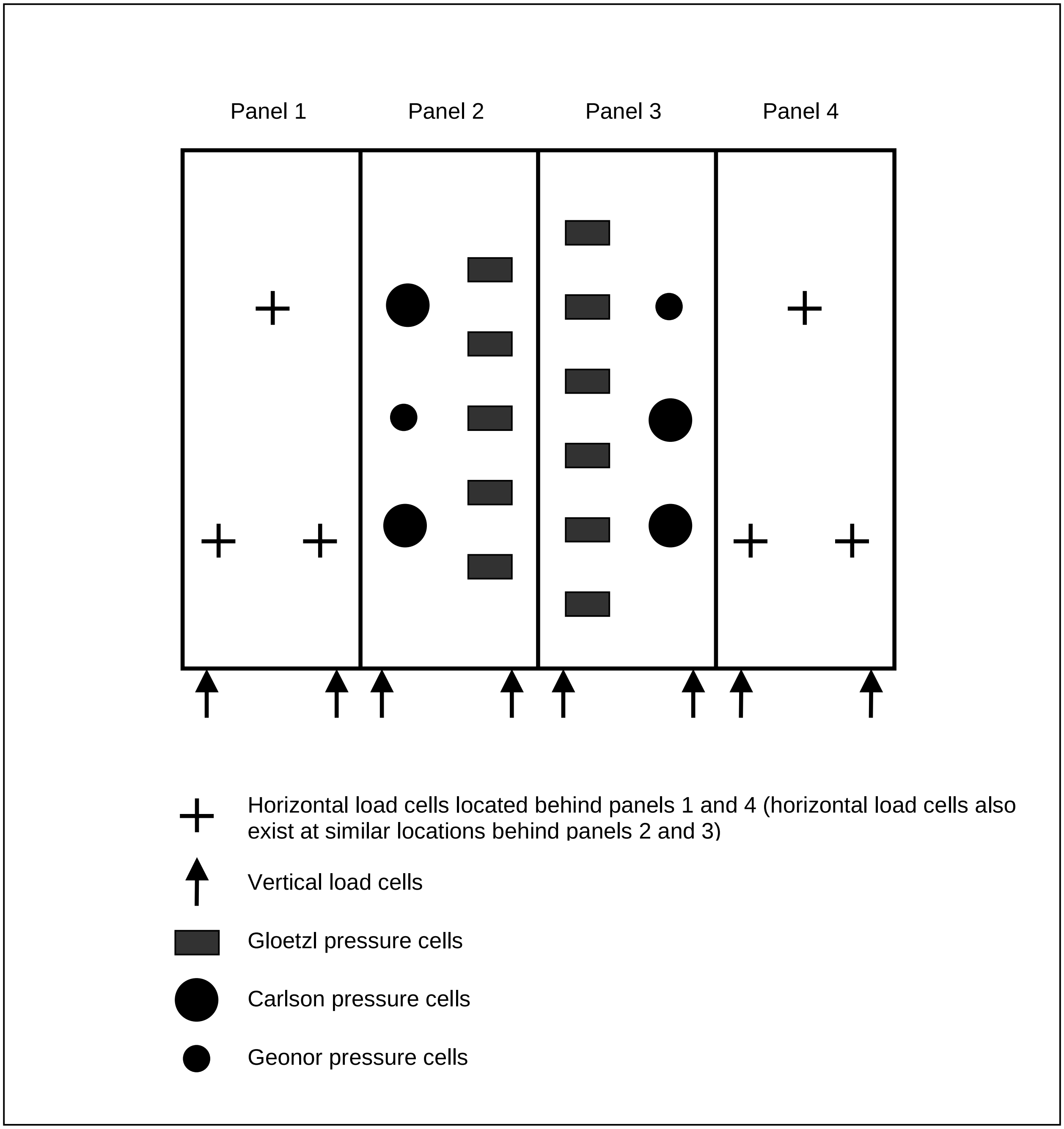

Figure 5-3. IRW panels (after Sehn 1990)

backfilling operations of the IRW provided qualitatively useful information on compaction-induced earth pressures.

A series of thermocouples are installed on both sides of the instrumented wall. The thermocouples provide data necessary for corrections of pressure and deformation readings, which may be needed when large temperature fluctuations take place during the test.

5.1.2 Preparations for the test

Simulation of a lock wall in the IRW required compaction of the backfill, application of a surcharge on the backfill surface, and inundation of the backfill. The IRW was not originally designed for surcharge application and inundation of the backfill. This section contains a description of the work performed to accommodate this type of testing in the IRW.

5.1.2.1 Construction of Bulkhead. To allow full inundation of the backfill, a bulkhead was built at the bottom of the access ramp. The bulkhead consisted of a rigid, wooden frame capable of withstanding the earth pressures generated during compaction, surcharge, and inundation. A 19-mm- (3/4-in.-) thick plywood facing was attached to the bulkhead on its backfill side. The bulkhead was pre-assembled outside the IRW and laid in place using the overhead crane. Tight tolerances were required to minimize the width of the gaps between the bulkhead and the existing concrete walls. The bulkhead was tightly attached to the walls and floor of the ramp with fifteen 12.5-mm- (1/2-in.-) steel bolts.

5.1.2.2 Water-seal. In order to prevent significant leaks during inundation of the backfill, a sealant was applied to all the gaps existing between the instrumented panels, between the panels and the floor, and along the edges of the bulkhead. All the gaps had a maximum width of approximately 12.5 mm (0.5 in.). Caulking strips were introduced in all gaps to serve as support for the sealant. A polyurethane-based, elastomeric sealant (Sikaflex-1a) was applied over the support strips with a thickness of approximately 12.5 mm (0.5 in.), and left to cure for 1 week. Once cured, the sealant has a relatively high strength and an elastic modulus ranging from 0.275 to 0.551 MPa. Application of the sealant to the bottom gap of the panels may have some influence on the force measurements of the load cells. However, this influence is minimal because the elastic modulus of the sealant is comparatively small, as confirmed by measurements performed before and after application of the sealant.

5.1.2.3 Inundation/drainage system. A simple system was devised to allow controlled inundation and drainage of the backfill. Two Polyvinyl Chloride (PVC) pipes were placed in the corners of the backfill area farthest from the instrumented panels. The pipes had an internal diameter of 150 mm (6 in.) and were approximately 2.5 m (8 ft) long. The pipes were perforated and entirely covered with a geotextile fabric. In this way, inundation and drainage were possible without causing migration of fines from the soil.

One of the pipes, referred to herein as the *well pipe*, was selected for introduction and removal of the water during inundation and drainage. The other pipe, referred to herein as the *piezometer*, was used to monitor the water level inside the backfill. For drainage of the backfill, a submersible electrical pump was introduced into the well pipe.

5.1.2.4 Data acquisition. A data acquisition system was installed in the IRW consisting of a Keithley 500A system connected to a personal computer equipped with a 486 processor. The Keithley 500A system allows use of up to ten 16-bit data acquisition cards designed for specific types of instrumentation. Table 5-1 lists some details regarding the data acquisition setup for the lock wall simulation.

Table 5-1
Features of the Data Acquisition System for the Lock Wall Simulation

Instruments	Card type	Voltage Range	Accuracy	Sampling Frequency Hz
Horizontal load cells	AIMM3a	±0.01 V	±0.22 kN	5
Vertical load cells	AIMM3a	±0.05 V	±0.07 kN	5
Gloetzl pressure cells	AIMM3a	±0.05 V	Not determined	5
LVDTs	AMM2	±0.5 V	±0.01 mm	5
Thermocouples	AMM7	±0.25 ^{o}C	±0.01 V	0.2

The data acquisition software provided with the Keithley 500 allows sampling of the instrumentation according to a predetermined sequence and sampling frequency. The digital output from the cards is converted into physical quantities according to calibration factors determined before the test. The software also allows graphic representation of the data.

The instruments were calibrated in situ before the test. The vertical and horizontal load cells were calibrated by the incremental application of forces of known magnitude at the load cell locations. Calibration of the load cells was verified after application of the sealant around the edges of the panels. It was found that the load absorbed by the sealant was negligible compared to the total loads applied to the panels. The Gloetzl pressure cells and LVDTs were calibrated following the procedures described by Sehn and Duncan (1990).

Several loading cycles were applied to the load cells and pressure cells to verify the repeatability of the measurements. No calibration was required for the thermocouples.

5.2 Testing Procedures

As illustrated in Figure 5-4, the test was performed in three stages:

a. Stage 1, backfilling.

b. Stage 2, surcharge.

c. Stage 3, inundation.

The following sections describe each of the stages of the test.

5.2.1 Stage 1, backfilling

Before the start of the backfilling operation, a nonfrictional lining was applied to the fixed walls and the bulkhead to minimize boundary effects. The lining consisted of an automotive grease coating and plastic film. Care was taken to avoid contaminating the surface of the instrumented panels or the floor of the backfill area during this process.

The backfill material was Light Castle Sand. The properties of Light Castle Sand are presented in Chapter 3, and Appendices A and B. The sand was air-dried to a water content below 0.2 percent, and stored inside the building until the start of the backfilling operation. The backfill was placed and compacted in 14 lifts, each with a compacted thickness of approximately 150 mm as illustrated in Figure 5-4. The sand was poured into the IRW using a hopper with bottom discharge as shown in Figure 5-5a. The weight of each batch of soil was carefully measured and recorded before pouring.

Each lift was compacted with two passes of a vibrating plate compactor as shown in Figure 5-5b. The compactor was a hand-operated Wacker model BPU2440A. After compaction of each lift, the total backfill thickness was determined by measuring the distance from the top of the backfill to a reference beam at twelve points distributed on the backfill surface. The thickness of the backfill was calculated based on the average of these readings. Measurements of horizontal and vertical forces, normal stresses, deformations, and temperatures were made after placement and after compaction of each lift.

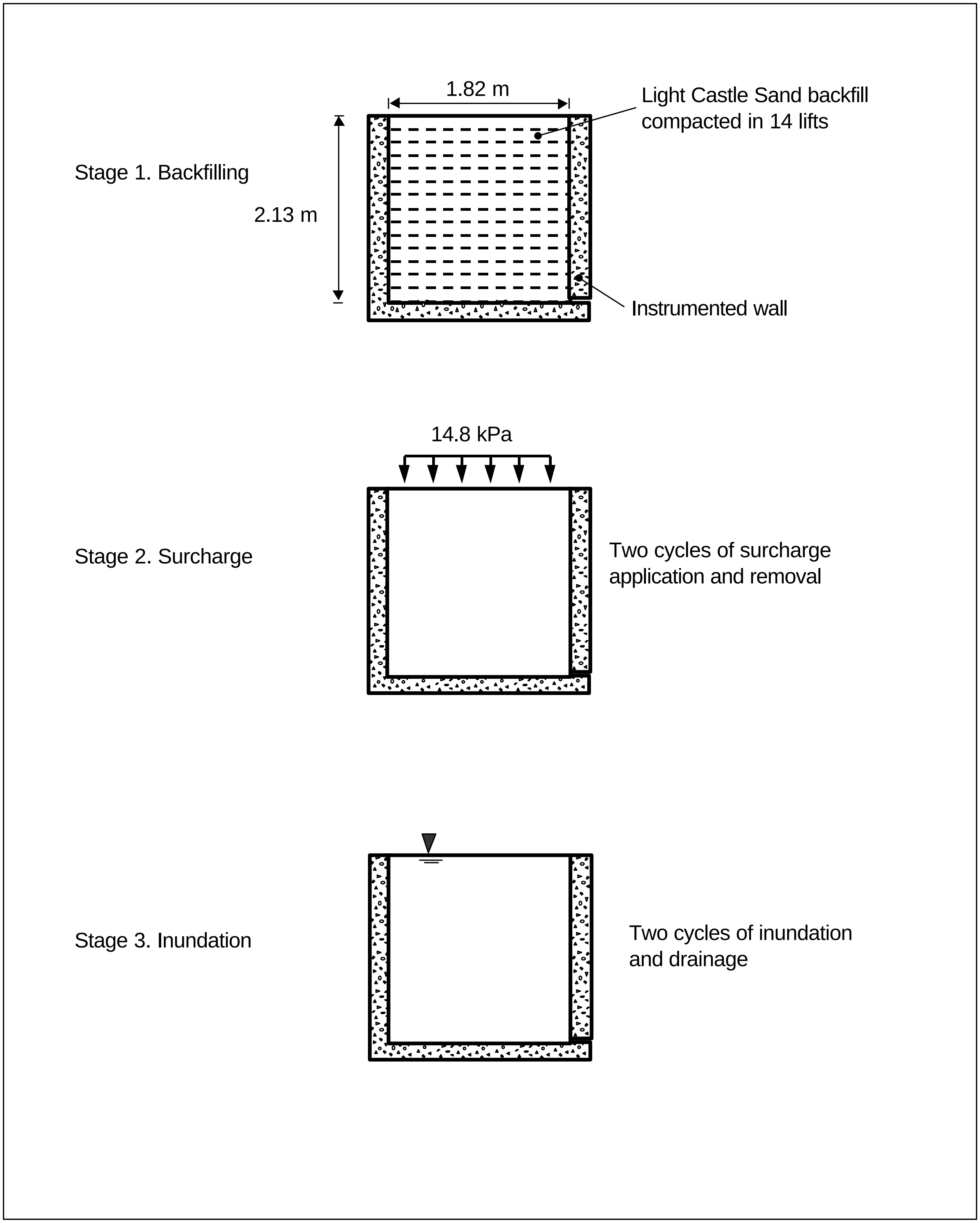

Figure 5-4. Stages of the lock wall simulation performed in the IRW test facility

a. Backfill placement b. Backfill compaction c. Surcharge application

Figure 5-5. View of the IRW at different stages of the lock wall simulation

The average density of the backfill at the end of compaction was 16.8 kN/m^3 (107 lb/ft^3), which corresponds approximately to the maximum density determined in the laboratory (Table 3-1). Previous investigators reported slightly lower density values for the Light Castle Sand backfill in the IRW following identical compaction procedures (Filz 1992). It is possible that the confinement provided by the wooden bulkhead helped to increase the compacted density of the backfill above the previous value. As discussed in a subsequent section, a beneficial consequence of the large backfill density was the minimization of hydrocompression effects during inundation.

5.2.2 Stage 2, surcharge

After completion of the backfilling operation, a surcharge was placed on the surface of the backfill. The surcharge consisted of a 1.07-m (3.5-ft) wooden container filled with Light Castle Sand in a loose condition. Figure 5-5c is a view of the IRW during application of the surcharge. The total weight of the sand plus the container induced a vertical pressure on the backfill surface of 14.8 kPa (310 lbf/ft^2).

Two cycles of placement and removal of the surcharge were applied. After the box was carefully placed on the surface of the backfill, it was filled with sand. A uniform, horizontal surface was kept during filling to maintain a uniform surcharge on the backfill. After completion of the surcharge application, the sand was slowly removed from the box through a side opening. An identical procedure was followed for the second cycle. A precise record of the weight of sand inside the box was kept during this stage of the test. Instrumentation readings were made before, during, and after each loading cycle.

5.2.3 Stage 3, inundation

Inundation of the backfill followed removal of the surcharge. After full inundation of the backfill, a submersible pump was introduced in the well pipe for drainage of the backfill. Two cycles of inundation and drainage were performed.

Instrumentation readings were made at several intermediate stages during inundation and drainage. Prior to each reading, the flow of water was arrested, and the water level in the pipes was monitored until equilibrium was reached. This prevented errors in the measurement of the water level inside the backfill.

Careful monitoring of flow rates during the test made possible estimation of the rate of leakage through the instrumented wall. It was found that the rate of leakage was negligible for practical purposes.

5.3 Test Results

The results of the test are summarized in Tables 5-2 to 5-5. Al the data reported in the tables correspond to measurements in the two central panels (panels 2 and 3) of the instrumented wall. It is assumed that panels 2 and 3 are relatively free from any significant boundary effects induced by the presence of the endwall and the bulkhead in the IRW. Consequently, data from these panels may most closely represent a plane strain condition that can be modeled with SOILSTRUCT-ALPHA. This section discusses the results obtained from each of the three stages of the test.

5.3.1 Results from stage 1

5.3.1.1 Force measurements. Table 5-2 summarizes the vertical and horizontal force data measured in the two central panels during compaction of the backfill. The data collected after placement and before compaction of each lift have been omitted for clarity. Measurements were made before and after any interruptions of the backfill placement process. They are also included in the table. The total horizontal and total vertical loads per panel correspond to the sum of the individual load cells readings in each panel. The effective overburden values are determined using Equation 1-1. The values of F'_x and F_v correspond to the horizontal and vertical forces, respectively, per unit length of wall. Definitions of the earth pressure coefficients, K_h and K_v, are presented in Chapter 1. According to Equations 1-2 and 1-3, the values of K_h and K_v are calculated by dividing the values of F'_x and F_v, respectively, by the effective overburden.

Table 5-2
Summary of the Force Measurements during Stage 1 of the IRW Test (Backfilling)[1]

Height of Backfill H m	Total Horizontal Load per Panel[2] kN		Total Vertical Force per Panel[2] kN		Effective Overburden kN / m	F'_x kN/m	F_v kN/m	K_h	K_v
	Panel 2	Panel 3	Panel 2	Panel 3					
0.00	0.000	0.000	0.000	0.000	0.000	0.000	0.000	-	-
0.15	0.096	0.126	0.027	-0.001	0.195	0.146	0.017	0.747	0.086
0.30	0.527	0.643	0.143	0.115	0.781	0.767	0.169	0.982	0.217
0.46	0.671	1.057	0.037	0.008	1.757	1.134	0.030	0.645	0.017
0.61	1.166	1.640	-0.083	-0.057	3.124	1.841	-0.091	0.589	-0.029
0.76	1.827	2.514	0.240	0.143	4.881	2.848	0.251	0.583	0.051
0.91	2.362	3.190	0.271	0.146	7.029	3.643	0.274	0.518	0.039
1.07	3.151	3.852	0.355	0.265	9.567	4.596	0.407	0.480	0.043
1.22	4.139	4.736	0.584	0.505	12.495	5.824	0.715	0.466	0.057
1.37	5.115	5.646	0.847	0.769	15.814	7.061	1.060	0.446	0.067
1.52	6.245	6.923	1.315	1.191	19.524	8.640	1.644	0.443	0.084
1.52	6.459	6.984	1.419	1.313	19.524	8.821	1.793	0.452	0.092
1.68	7.988	8.447	1.838	1.681	23.624	10.785	2.309	0.457	0.098
1.83	9.031	9.598	2.227	2.067	28.114	12.224	2.818	0.435	0.100
1.98	10.420	10.499	2.734	2.486	32.995	13.726	3.425	0.416	0.104
2.13	11.478	11.562	3.191	2.936	38.266	15.118	4.020	0.395	0.105
2.13	11.222	11.394	3.183	2.904	38.266	14.840	3.994	0.388	0.104

[1] See Notation (Appendix F) for definition of symbols.
[2] Measurements made after placement and before compaction of each lift are omitted.

It can be observed that the magnitudes of vertical and horizontal forces are similar for the two panels. They are also similar to the values reported by Filz (1992) for a previous IRW test using the Light Castle Sand backfill.

5.3.1.2 Pressure measurements. The data from the Gloetzl pressure cells at the end of backfilling are presented in Table 5-3. Integration of these pressure values over the height of the wall yields a horizontal force magnitude of 17.35 kN per meter run of wall. This value is approximately 17 percent greater than the value of 14.84 kN/m obtained from the load cell measurements presented in Table 5-2. Table 5-3 also shows the corrected values of normal pressure, which were obtained by dividing the pressure data by 1.17.

Table 5-3 Data From Gloetzl Pressure Cells at the End of Stage 1 (Backfilling)			
Gloetzl Cell Number	**Position of Cell[1] m**	**Horizontal Pressure, σ_h kPa**	
		Measured	**Corrected [2]**
G1	1.778	12.44	10.64
G7	1.626	11.29	9.65
G2	1.473	8.83	7.55
G8	1.321	No response	-
G3	1.168	10.20	8.72
G9	1.016	9.76	8.34
G4	0.864	8.31	7.11
G10	0.711	10.15	8.68
G5	0.559	9.53	8.15
G11	0.406	8.48	7.25
G6	0.253	No response	-

[1] Measured from bottom of backfill to center of each cell.
[2] Obtained by dividing the measured pressure by 1.17.

The magnitude of the error in the pressure measurements suggests that Gloetzl cells do not provide data that is usable for accurate analyses of the response of the wall-backfill system. However, they provide an important insight for SSI analyses of the IRW, as discussed in the section on the interpretation of the test results.

5.3.2 Results from stage 2

Table 5-4 summarizes the data from the two cycles of application and removal of the surcharge. The vertical force increment due to surcharge application $F_{v,q}$ and the vertical shear force coefficient for sloping backfill and surcharge $K_{v,q}$ are defined in Chapter 2. The value of $F_{v,q}$ is the difference between the values of F_v after and before the application of the surcharge q_s. Rearranging terms in Equation 2-16 gives the following expression for the determination of $K_{v,q}$ from the IRW data:

$$K_{v,q} = \frac{F_{v,q}}{q_s \cdot H} \tag{5-1}$$

The magnitudes of the vertical shear load before and after this stage of the test are very similar. This suggests that there is little or no degradation of the vertical shear loads with cycles of application and removal of the surcharge.

Table 5-4 **Summary of the Results of Stage 2 of the IRW (Surcharge)**[1]								
Applied Surcharge, q_s kPa	**Total Horizontal Load per Panel kN**		**Total Vertical Force per Panel kN**		**F'_x kN/m**	**F_v kN/m**	**$F_{v,q}$ kN/m**	**$K_{v,q}$**
	Panel 2	**Panel 3**	**Panel 2**	**Panel 3**				
0.0 [2]	11.22	11.39	3.18	2.90	14.84	3.99	0.000	-
0.3	11.31	11.63	3.21	2.95	15.05	4.04	0.048	0.079
0.3	11.82	11.97	3.35	3.10	15.61	4.23	0.236	0.388
9.2	12.67	13.76	4.11	4.00	17.34	5.32	1.324	0.067
18.2	13.32	14.91	4.86	4.81	18.52	6.35	2.351	0.061
0.3	10.75	11.07	3.49	3.25	14.32	4.42	0.427	0.704
18.2	12.82	13.56	4.99	4.75	17.30	6.39	2.397	0.062
18.2	13.03	13.60	5.03	4.80	17.48	6.45	2.459	0.063
0.00	10.86	11.05	3.48	3.23	14.38	4.40	0.411	-

[1] See Notation (Appendix F) for definition of symbols.
[2] Corresponds to end of backfilling (last row of Table 5-2).

5.3.3 Results from stage 3

5.3.3.1 Force measurements. The data collected during the inundation cycles of the IRW test are summarized in Table 5-5. The hydrostatic force on the wall F_w is calculated from the following expression:

$$F_w = \frac{\gamma_w \cdot D_2^{\,2}}{2} \qquad (5\text{-}2)$$

The effective horizontal force F'_x is calculated by subtracting the hydrostatic force F_w from the total horizontal force F_x. The definition of the correction factor C_{wt} for a post-construction rise in the water table was presented in Chapter 2. The value of C_{wt} for the IRW test was calculated as the ratio between the K_v values during inundation and the K_v value immediately before the start of inundation (Equation 2-20).

It can be seen that the magnitude of the vertical shear force F_v decreases as the height of water in the backfill D_2 increases during inundation. Conversely, the magnitude of F_v increases as D_2 decreases during drainage. Drainage of the backfill was carried out until D_2 reached a value of approximately 0.3 m. Further lowering of the water table was not practical because the time required for full drainage of the backfill (D_2 = 0) was too long. However, extrapolation of the vertical force data collected during the two drainage stages reveals that the value of F_v for full drainage (D_2 = 0) is similar to its initial value before the start of inundation (F_v = 4.40 kN/m). This suggests that there is no significant

Table 5-5
Summary of the Results of Stage 3 of the IRW (Inundation)[1]

Cycle		D_2 m	D_2 / H	D_1 m	F_w kN/m	Total Horizontal Force per Panel kN		Total Vertical Force per Panel kN		F_x kN/m	F'_x kN/m	F_v kN/m	K_v	C_{wt}
						Panel 2	Panel 3	Panel 2	Panel 3					
1	Inundation	0.00	0.00	2.13	0.00	10.86 [2]	11.05 [2]	3.48 [2]	3.23 [2]	14.38 [2]	14.38 [2]	4.40 [2]	0.115 [2]	1.000
		0.60	0.28	1.54	1.75	10.85	10.63	2.46	2.23	14.09	12.35	3.07	0.083	0.721
		0.95	0.45	1.18	4.45	12.04	11.69	1.79	1.43	15.57	11.13	2.11	0.060	0.522
		1.32	0.62	0.81	8.55	14.48	13.50	1.28	1.11	18.36	9.81	1.56	0.049	0.422
		1.52	0.71	0.61	11.38	15.67	14.90	1.12	1.08	20.06	8.68	1.44	0.048	0.416
		1.50	0.71	0.63	11.10	14.89	14.42	1.10	1.07	19.24	8.14	1.43	0.047	0.408
		1.83	0.86	0.30	16.39	17.54	16.46	0.81	0.92	22.31	5.92	1.13	0.043	0.371
		2.06	0.96	0.08	20.74	18.97	17.83	0.57	0.81	24.14	3.40	0.91	0.039	0.335
	Drainage	1.77	0.83	0.37	15.27	16.59	15.61	0.93	1.16	21.13	5.86	1.37	0.049	0.428
		1.60	0.75	0.53	12.55	15.15	14.10	0.94	1.13	19.19	6.65	1.36	0.045	0.394
		1.40	0.65	0.74	9.56	14.70	13.51	1.06	1.21	18.51	8.94	1.49	0.046	0.400
		1.19	0.56	0.94	6.98	13.83	12.51	1.34	1.49	17.29	10.31	1.86	0.054	0.470
		0.72	0.34	1.41	2.57	11.73	10.19	1.88	1.99	14.38	11.81	2.54	0.067	0.585
		0.65	0.30	1.49	2.06	11.87	10.15	1.83	1.91	14.45	12.39	2.45	0.064	0.560
		0.36	0.17	1.77	0.64	11.82	9.78	2.24	2.27	14.17	13.53	2.96	0.075	0.655
		0.33	0.15	1.80	0.53	11.57	9.25	2.55	2.55	13.66	13.13	3.35	0.085	0.741
2	Inundation	0.88	0.41	1.26	3.76	12.33	10.14	2.07	2.14	14.74	10.98	2.76	0.075	0.652
		1.70	0.80	0.43	14.19	16.86	15.17	1.18	1.40	21.02	6.83	1.70	0.059	0.514
		2.13	1.00	0.01	22.31	20.09	18.53	0.75	1.05	25.35	3.04	1.18	0.053	0.458
	Drainage	1.66	0.78	0.48	13.46	16.66	14.91	1.16	1.39	20.71	7.25	1.67	0.057	0.497
		1.11	0.52	1.02	6.05	13.76	12.11	1.93	2.06	16.97	10.92	2.62	0.075	0.650
		0.61	0.29	1.52	1.82	11.81	10.07	2.52	2.65	14.36	12.54	3.39	0.089	0.770
		0.32	0.15	1.81	0.51	12.01	9.83	2.93	3.03	14.33	13.82	3.91	0.099	0.864

[1] D_1 = thickness of backfill above the water table, D_2 = height of water behind the wall, F_w = hydrostatic force on wall, F_x = total horizontal force. See Notation (Appendix F) for definitions of other symbols.
[2] Corresponds to end of surcharge cycle (last row of Table 5-4)

degradation of the vertical shear force with cycles of inundation for the conditions of this test in the IRW.

5.3.3.2 Hydrocompression. During inundation, the elevation of the surface of the backfill was measured periodically with an accuracy of ±1 mm. No significant changes in the backfill height were detected during inundation. This is consistent with the analysis of the hydrocompression properties of the Light Castle Sand presented in Appendix A. Therefore, for the analyses of the IRW, it was assumed that hydrocompression of the backfill is negligible.

5.4 Discussion of Test Results

In this section, the backfill response observed during the test and its relevance for the finite element analyses of the IRW are discussed.

5.4.1 Response of the wall-backfill system to backfilling

5.4.1.1 Evolution of lateral earth pressures during backfilling. The values of the lateral earth pressure coefficient K_h, listed in Table 5-2, are plotted against the height of the backfill in Figure 5-6. It can be seen that the value of K_h decreases as the height of the backfill increases. A value of K_h of approximately 0.4 was obtained at the end of backfilling.

For comparison, the value of the at-rest coefficient K_o determined using the approximation suggested by Jaky (1948) for an internal friction angle of the backfill of 47 deg, is also illustrated in the figure. The at-rest coefficient does not account for compaction-induced lateral earth pressures behind walls with rough interfaces. Therefore, the value of K_o should be identical to the value of K_h in a nonmoving wall retaining a normally consolidated backfill and with a smooth backfill-to-wall interface. The value of K_h in the IRW is larger than the value of the at-rest coefficient throughout the backfilling stage because significant lateral stresses are locked in during compaction of the backfill.

Figure 5-7 shows the pressure distribution at the end of backfilling in the IRW test. Data from a similar test performed previously in the IRW (Filz 1992) are also shown. It can be seen that the pressure distribution on the wall is not linear and that large horizontal pressures develop throughout the height of the wall. As discussed by Duncan et al. (1991), compaction-induced earth pressures are much greater than the at-rest values near the surface of a compacted backfill. At large depths, the overburden pressure induced by the weight of the overlying backfill is significantly larger than the vertical stresses applied during compaction. Therefore, in short walls such as the IRW, the magnitude of the total horizontal force on the wall may be controlled by compaction-induced earth pressures.

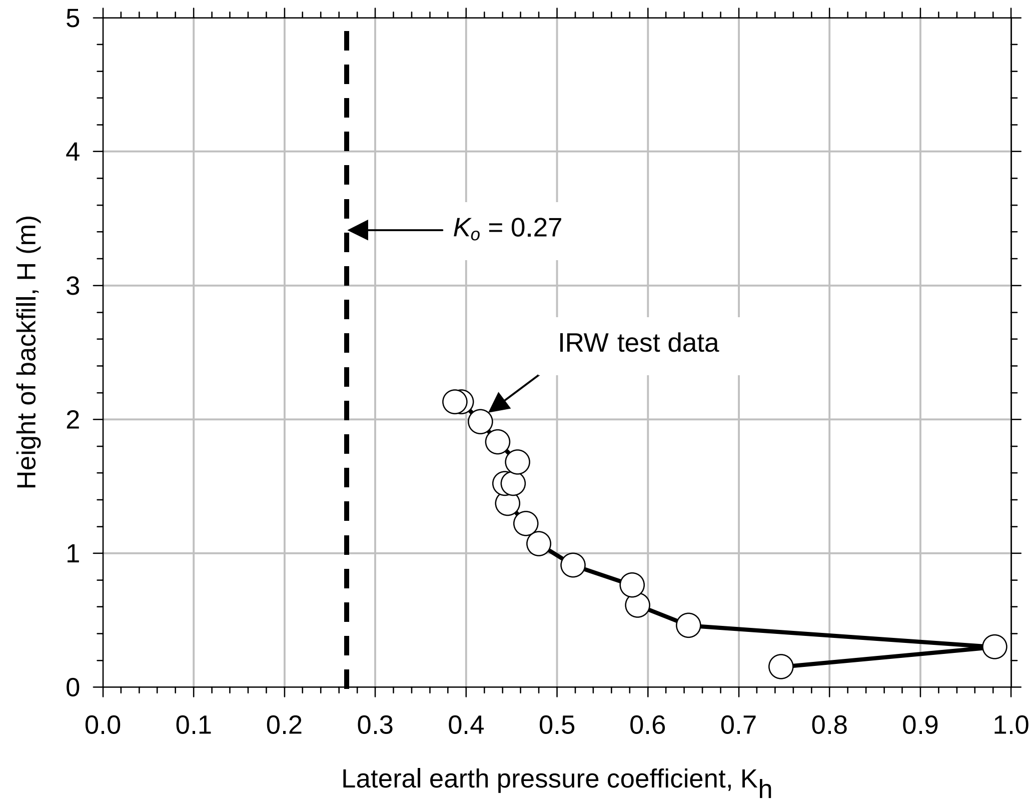

Figure 5-6. Evolution of the lateral earth pressure coefficient, K_h, during backfilling in the IRW

In higher walls, the total horizontal force on the wall may be controlled by the at-rest pressures for normally consolidated soil backfills. As the height of the backfill increases, the value of K_h decreases. For lock walls, which are typically 12 m (40 ft) or higher and have smooth wall-to-backfill interfaces, the K_h values approach Jaky's K_o value, since the stresses induced by the overburden exceed the stresses induced by compaction.

To perform accurate analyses of short walls such as the IRW, it is necessary to account for the relatively large pressures that develop at shallow depths inside the backfill.

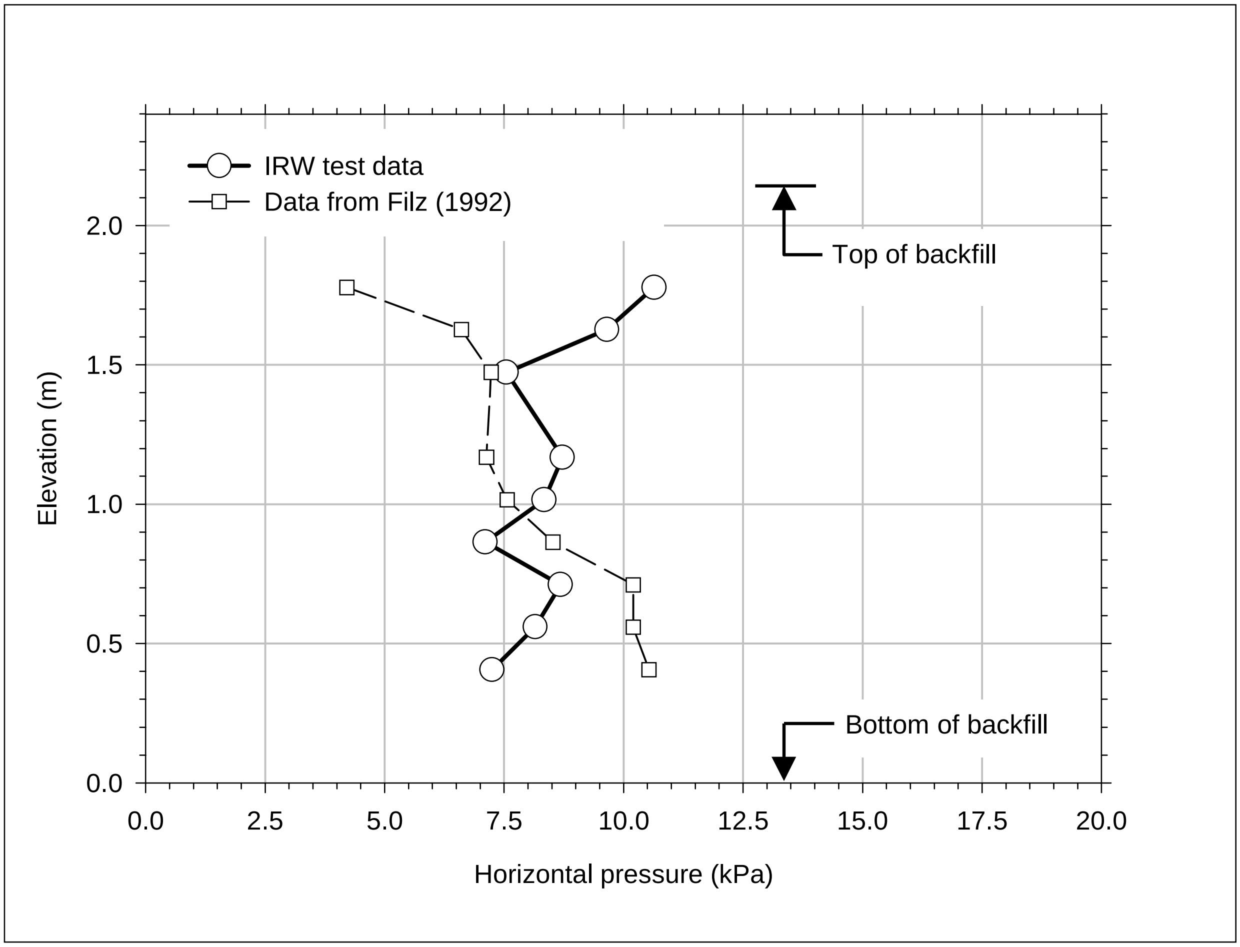

Figure 5-7. Lateral pressure distribution at the end of backfilling

5.4.1.2 Evolution of vertical shear forces during backfilling. The values of the vertical force coefficient K_v, measured during stage 1 of the test, are plotted in Figure 5-8 against the height of the backfill. The value of K_v increases with the height of the backfill to a final value of approximately 0.10 at the end of backfilling. This value is consistent with the results of a previous test performed in the IRW (Filz 1992).

A discussion of the development of vertical shear forces in nonmoving walls was presented by Filz and Duncan (1997) and Filz, Duncan, and Ebeling (1997). From a series of finite element analyses, they developed a set of K_v versus backfill height curves for different densities of the backfill. Figure 2-6 reproduces the results of their analyses. The calculated values of K_v for dense, granular backfills are reproduced in Figure 5-8, together with the design line recommended in Appendix F of Engineer Manual 1110-2-2100 (HQUSACE, in preparation).

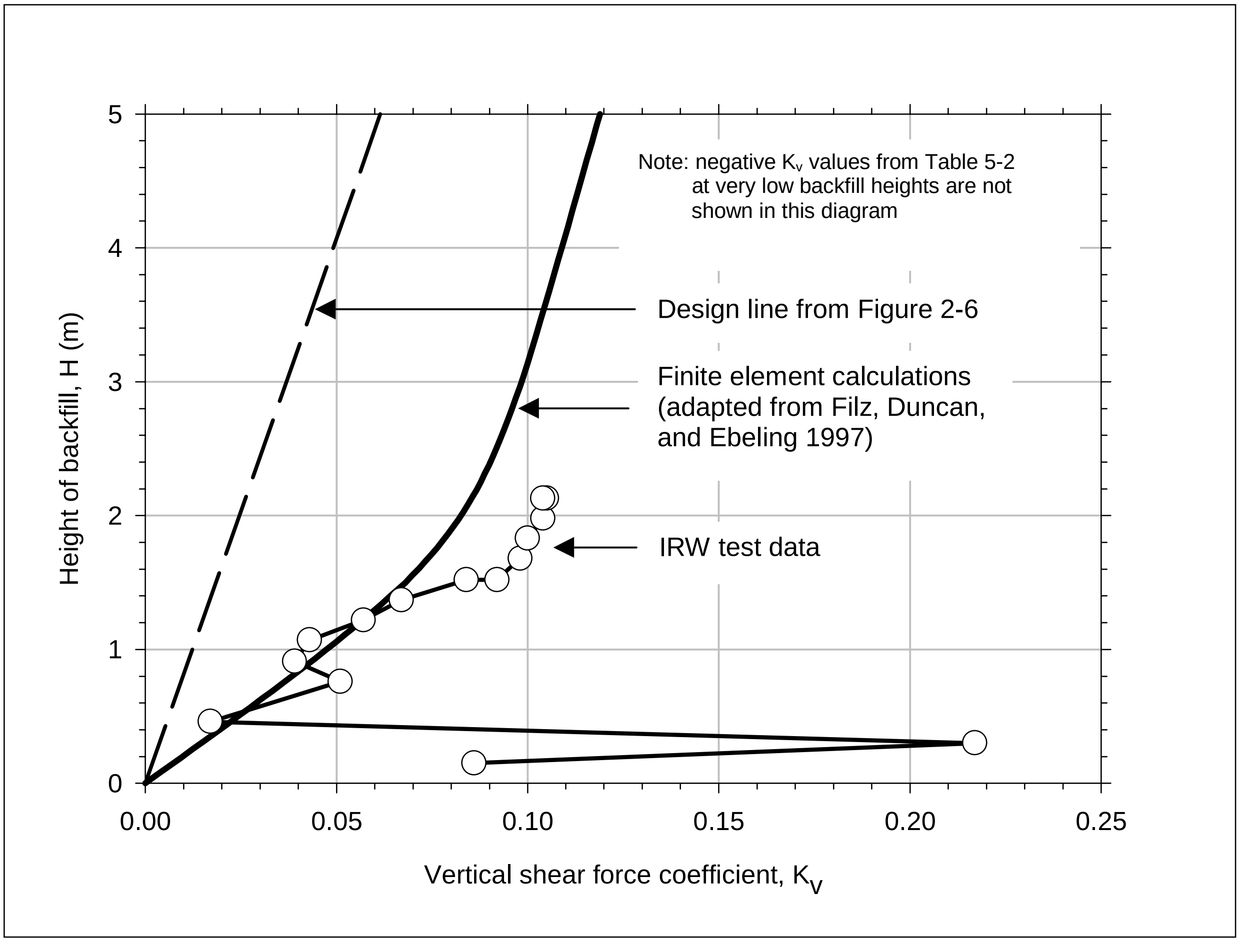

Figure 5-8. Evolution of the vertical shear force coefficient, K_V, during backfilling in the IRW

It can be observed that the calculated and measured K_v values follow similar trends of variation with backfill height. However, the measured K_v values at the end of backfilling are somewhat higher than the calculated values.

The design line shown in Figure 5-8 provides conservative estimates of K_v, according to the IRW data.

5.4.2 Response of the wall-backfill system to surcharge

Values of the earth pressure coefficient for surcharge $K_{v,\,q}$ determined from force measurements in stage 2 are listed in Table 5-4. Neglecting the extreme values for low surcharge magnitudes, the average value of $K_{v,\,q}$ is 0.063. In the IRW test, the backfill surface is horizontal and the distance from the surcharge to the wall is zero. Therefore, the concept of $K_{v,\,q}$ is equivalent to the concept of

$K_{v,q,ref}$ discussed in Chapter 2. The average value of $K_{v,\,q}$ from the test is represented in a $K_{v,\,q,\,ref}$ versus backfill height diagram in Figure 5-9.

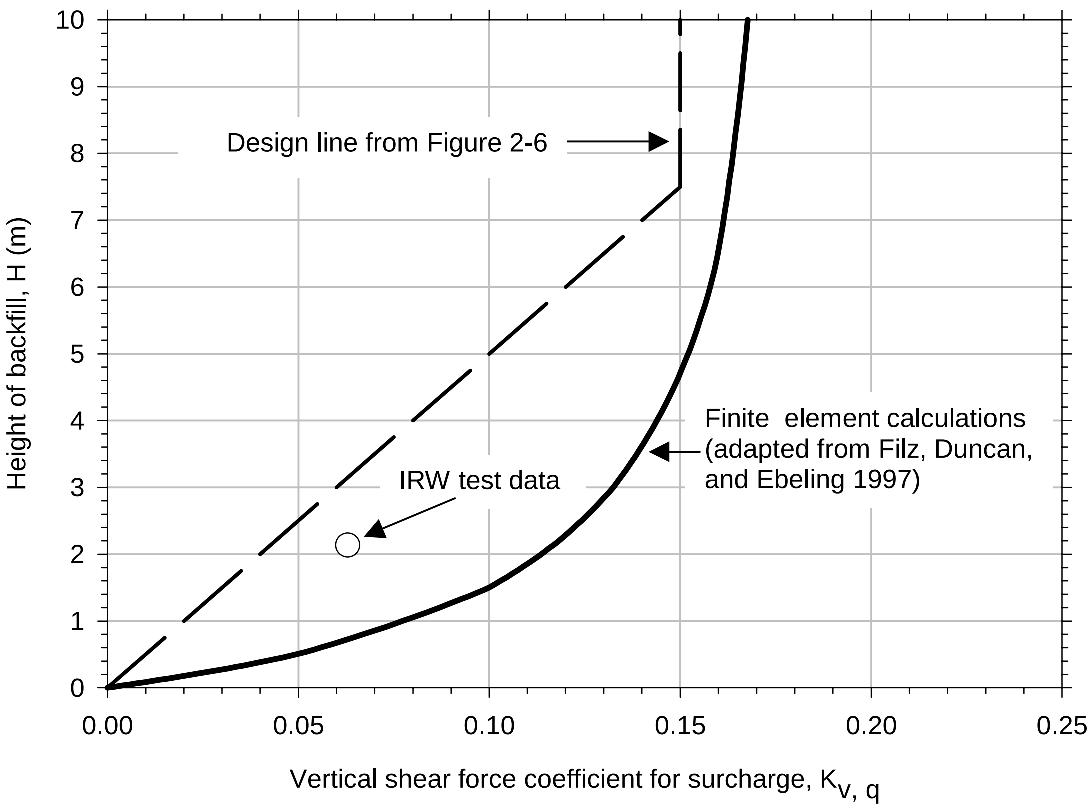

Figure 5-9. Vertical shear force coefficient for surcharge, $K_{v,\,q}$, in the IRW

The $K_{v,\,q}$ values obtained by Filz, Duncan, and Ebeling (1997) from finite element analyses of nonmoving walls with dense backfills are also represented in Figure 5-9. These analyses were performed using the same backfill properties as those used in their backfilling analyses discussed in the previous section. From the theoretical plots, a value of $K_{v,\,q}$ of approximately 0.12 is obtained. This value is larger than the $K_{v,\,q}$ value determined from the IRW data. This difference between calculated and measured $K_{v,\,q}$ values occurs because the compressibility of the backfill assumed for the analyses is larger than the compressibility of the compacted Light Castle Sand, as discussed in Sections 5.5.3 and 5.6.2.

The design line recommended in Appendix F of Engineer Manual 1110-2-2100 (HQUSACE, in preparation) is also reproduced in Figure 5-9. It provides a slightly conservative estimate of the value of $K_{v,\,q}$, according to the IRW data.

5.4.3 Response of the wall-backfill system to inundation

The values of the correction factor C_{wt} listed in Table 5-5 are plotted against the normalized height of water D_2/H in Figure 5-10. The test data follow a curvilinear path reaching an average final value of C_{wt} of approximately 0.4 after full inundation of the backfill (D_2/H = 1). The design line recommended in Appendix F of Engineer Manual 1110-2-2100 (HQUSACE, in preparation) is also represented in the figure. It yields a good approximation to the C_{wt} values from the IRW test for D_2/H ratios lower than 0.5. For D_2/H ratios between 0.5 and 1, the design line yields conservative values of the correction factor.

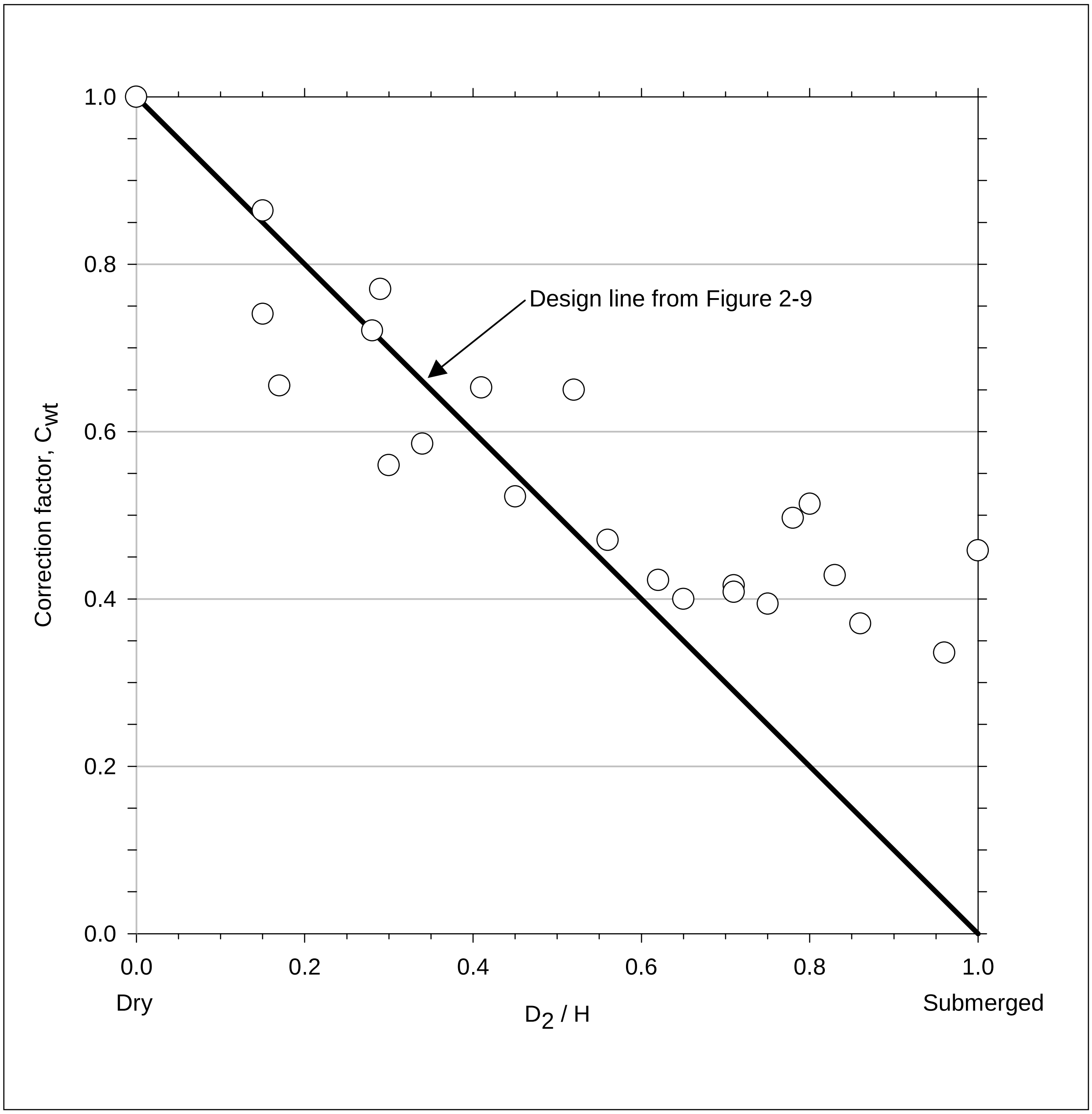

Figure 5-10. Values of the correction factor, C_{wt}, during inundation of the backfill in the IRW

5.4.4 Special considerations for finite element analyses of the IRW

A method to incorporate compaction effects into finite element analyses was developed by Seed and Duncan (1986). The compaction of each lift was modeled as the temporary application of compaction stresses on the surface of the backfill. They used a hysteretic soil model, which provided reasonable estimations of the residual earth pressures after removal of the compaction stresses.

The implementation of such a model in SOILSTRUCT-ALPHA may be a lengthy process, and it is beyond the scope of this investigation. Therefore, a simpler, alternative procedure was followed to model the response of the wall-backfill system to all types of loading applied during the test. For the analyses, different backfill property values were assigned for backfilling than those assigned for surcharge placement. The effect of compaction on the lateral pressures was modeled by assigning a larger Poisson's ratio and a lower modulus to the backfill material for stage 1 (backfilling) than for stage 2 (surcharge).

In previous sections of this report, it was observed that at the end of backfilling in the IRW, large horizontal pressures exist throughout the height of the instrumented wall, and that the pressure distribution is not linear with depth. To obtain accurate values of vertical and horizontal forces from finite element analyses of the IRW, it is necessary to account for this type of lateral pressure distribution. Finite element analyses in SOILSTRUCT-ALPHA do not provide the type of horizontal pressure distribution observed in the IRW test. In the analyses, the distribution tends to be linear, and pressures are low at shallow depths in the backfill. Consequently, the effect of the confining pressures on the backfill response to loading is not accurately modeled in the analyses. Additional adjustments of the backfill properties are required to account for the larger confining pressures that occur due to compaction.

For these reasons, limited information on the accuracy of the extended hyperbolic model can be expected from the analyses of the IRW for the backfilling and surcharge stages. The analyses of stages 1 and 2 were performed to obtain a reasonable estimate of the backfill properties and of the state of stresses existing prior to inundation. The backfill properties and state of stresses obtained from these calibration analyses were used for the analysis of inundation. The comparison between the results of the inundation analysis and the test data is the basis for the evaluation of the extended hyperbolic model.

These issues regarding the limitations of SOILSTRUCT-ALPHA analyses of the IRW may not be applicable to most lock walls. In lock walls of moderate to large height, the earth pressures are largely controlled by the self-weight of the backfill. A single set of material properties that produces reasonable estimates of earth pressures for backfilling may also produce reasonable estimates for surcharge application and for post-construction rise of the groundwater table.

5.5 Finite Element Analysis Procedures

Finite element analyses were performed to model the IRW test using the updated version of the program SOILSTRUCT-ALPHA, which contains the extended hyperbolic model presented in Chapter 4. The following steps were followed for the analyses:

a. Selection of tentative material properties for the backfill.

b. Calibration analyses.

c. Inundation analysis.

Tentative values of backfill properties were determined from the results of the triaxial and consolidation tests on the Light Castle Sand. These values were adjusted during the calibration analyses to match the force values measured at the end of the backfilling and surcharge stages. Finally, these adjusted properties were used for the analyses of the inundation stage.

This section summarizes the features of SOILSTRUCT-ALPHA that are relevant for the analyses performed. The criteria followed for the selection of the material property values and procedures used for the calibration and backfill inundation analyses are described in detail. Finally, the analysis results are compared to the data collected during the IRW test, and the accuracy of the extended hyperbolic model for interfaces is discussed.

5.5.1 Summary of features of SOILSTRUCT-ALPHA

The program SOILSTRUCT was developed by Clough and Duncan (1969) for finite element analyses of earth retaining structures. It is a general-purpose finite element program for two-dimensional analysis of plane strain problems of soil-structure interaction. It calculates stresses and displacements due to incremental construction and/or load application, and can model nonlinear stress-strain material behavior. Two types of finite elements are used in SOILSTRUCT: two-dimensional elements for soil and structural materials, and joint elements for the interfaces between the different materials. SOILSTRUCT has undergone a continuous evolution as new developments have been introduced in soil and interface models. SOILSTRUCT-ALPHA is the latest result of this process (as described in Ebeling and Wahl 1997 and Ebeling, Pace, and Morrison 1997).

In SOILSTRUCT-ALPHA, the nonlinear response of soils to primary loading is modeled using the hyperbolic formulation by Duncan and Chang (1970). For unloading-reloading, a stress-dependent, linear response is assumed

(Ebeling, Peters, and Clough 1992). The Alpha method (Ebeling, Duncan, and Clough 1990; Ebeling et al. 1992) implemented in the code allows analyses of lock walls undergoing base separation. Base separation is not a relevant issue for the IRW analyses, and it is not discussed further in this report.

As indicated in Chapter 4, the updated version of SOILSTRUCT-ALPHA, which was developed during this investigation, contains the formulation for yield-inducing shear and unloading-reloading Version II of the extended hyperbolic model for interfaces.

5.5.1.1 Incremental analysis techniques. In SOILSTRUCT-ALPHA, analyses are performed following the incremental techniques described by Clough and Duncan (1969). In the analyses, the backfill elements and structure-to-backfill interface elements take on three different states during the analyses: air, fluid, and solid. In the initial condition before the start of backfilling, all the backfill and interface elements are assigned the properties of air and of structure-to-air interface, respectively.

Each newly placed lift is modeled as a dense fluid, with a unit weight equal to the unit weight of the compacted backfill. The pressures exerted by the new lift on the existing backfill and on the structural elements are calculated and transformed into nodal loads. The interface elements between the structure and the newly placed lift are assigned a low value of shear stiffness and, as discussed in Chapter 2, a large value of normal stiffness. Zero nodal displacements are prescribed at the surface of the newly placed lift to prevent buildup of displacements in the overlying air elements.

The value of the at-rest pressure coefficient K_o assigned to the fluid elements is usually assumed equal to one. It determines the magnitude of the lateral pressures between the fluid elements and between the fluid elements and the retaining wall.

Upon addition of subsequent lifts to the mesh, the previously fluid elements take on a solid state. At this time, the complete set of properties of the compacted backfill and of the structure-to-backfill interface are assigned to the backfill and interface elements.

For soil and backfill, the incremental changes in stresses are related to the incremental strains through the linear relationship:

$$\begin{Bmatrix} \Delta\sigma_x \\ \Delta\sigma_y \\ \Delta\tau_{xy} \end{Bmatrix} = \frac{3 \cdot B}{9 \cdot B - E_t} \begin{bmatrix} (3 \cdot B + E_t) & (3 \cdot B - E_t) & 0 \\ (3 \cdot B - E_t) & (3 \cdot B + E_t) & 0 \\ 0 & 0 & E_t \end{bmatrix} \cdot \begin{Bmatrix} \Delta\varepsilon_x \\ \Delta\varepsilon_y \\ \Delta\gamma_{xy} \end{Bmatrix} \tag{5-3}$$

where

$\Delta\sigma_x$ = horizontal stress increment

$\Delta\sigma_y$ = vertical stress increment

$\Delta\tau_{xy}$ = shear stress increment

B = bulk modulus of the soil

E_t =tangent modulus of the soil

$\Delta\varepsilon_x$ = horizontal strain increment

$\Delta\varepsilon_y$ = vertical strain increment

$\Delta\gamma_{xy}$ = shear strain increment

For interface elements, the incremental changes in stresses and displacements are related according to the following expression:

$$\begin{Bmatrix} \Delta\tau \\ \Delta\sigma_n \end{Bmatrix} = \begin{bmatrix} K'_{st} & 0 \\ 0 & K_n \end{bmatrix} \cdot \begin{Bmatrix} \Delta_s \\ \Delta_n \end{Bmatrix} \tag{5-4}$$

where

$\Delta\tau$ = shear stress increment

$\Delta\sigma_n$ = normal stress increment

K'_{st} = tangent shear stiffness of the interface

K_n = interface normal stiffness

Δ_s = interface shear displacement

Δ_n = interface normal displacement

5.5.1.2 Soil properties. The tangent Young's modulus E_t of the soil for use in each load increment is computed from the following equation:

$$E_t = E_i \cdot \left(1 - R_f \cdot SL\right)^2 \tag{5-5}$$

where

E_i = initial Young's modulus of the soil

R_f = failure ratio of the soil

SL = stress level

In effective stress analyses, the initial Young's modulus E_i is determined from

$$E_i = K \cdot p_a \cdot \left(\frac{\sigma'_3}{p_a}\right)^n \tag{5-6}$$

where

K = modulus number of the soil

n = modulus exponent of the soil

σ'_3 = minor effective principal stress

The stress level SL in soils is determined from:

$$SL = \frac{(\sigma_1 - \sigma_3)}{(\sigma_1 - \sigma_3)_f} \tag{5-7}$$

where

σ_1 = major principal stress

σ_3 = minor principal stress

For a frictional backfill with zero cohesion intercept, the deviator stress at failure $(\sigma_1\text{-}\sigma_3)_f$ is determined from:

$$(\sigma_1 - \sigma_3)_f = 2\frac{\sigma'_3 \cdot sin(\phi)}{1 - sin(\phi)} \tag{5-8}$$

where ϕ is the internal friction angle of the soil

In this formulation, the parameters K, n, R_f, and ϕ are the hyperbolic parameters defined by Duncan and Chang (1970) for modeling the response of the soil to primary loading. During unloading-reloading, a linear, stress-dependent soil response is assumed. The value of the Young's modulus E_{ur} for unloading-reloading is calculated from the following expression:

$$E_{ur} = K_{ur} \cdot p_a \cdot \left(\frac{\sigma'_3}{p_a}\right)^n \tag{5-9}$$

where K_{ur} is the unload-reload modulus number.

According to the hyperbolic formulation by Duncan and Chang (1970), the bulk modulus, B, of the soil is calculated from the equation:

$$B = K_b \cdot p_a \cdot \left(\frac{\sigma'_3}{p_a}\right)^m \tag{5-10}$$

where

K_b = bulk modulus number

m = bulk modulus exponent

In SOILSTRUCT-ALPHA, the following approximate formulation is used to calculate the bulk modulus number (Ebeling, Pace, and Morrison 1997):

$$K_b = \frac{K}{3 \cdot (1 - 2 \cdot \upsilon_{nom})} \tag{5-11}$$

In Equation 5-11, it is implicitly assumed that the values of modulus exponent *n* and the bulk modulus exponent *m* are identical. The nominal Poisson's ratio ν_{nom} is related to Poisson's ratio ν according to the following expression (Ebeling, Pace, and Morrison 1997):

$$\upsilon = \frac{1 - (1 - 2 \cdot \upsilon_{nom}) \cdot (1 - R_f \cdot SL)^2}{2} \tag{5-12}$$

The at-rest pressure coefficient K_o, used only for the analysis of the stresses induced by the newly placed lift, is usually assumed equal to one. The unit weight of the soil γ is assumed equal to the moist unit weight γ_{moist} for the portion of the backfill above the water table, and to the saturated unit weight γ_{sat} for the portion below the water table. Table 5-6 is a summary of the properties required to model soils in SOILSTRUCT-ALPHA analyses.

Table 5-6
Summary of Soil Properties Required in SOILSTRUCT-ALPHA Analyses

Soil Property	Definition
K	Modulus number
n	Modulus exponent
K_{ur}	Modulus number for unloading-reloading
R_f	Failure ratio
ϕ	Internal friction angle
ν_{nom}	Nominal Poisson's ratio
K_o	At-rest earth pressure coefficient for fluid backfill
γ_{moist}, γ_{sat}	Moist and saturated unit weight, respectively

5.5.1.3 Interface properties. The tangent shear stiffness K'_{st} of the interface is determined according to the formulations for yield-inducing shear and for unloading-reloading, Version II, of the extended hyperbolic model introduced in Chapter 4. The normal stiffness K_n is assigned a large value to minimize overlapping of adjacent elements in the mesh.

5.5.2 Finite element mesh

Figure 5-11 shows the mesh used for the finite element analyses of the IRW. It is composed of the following elements:

a. 224 two-dimensional elements for modeling the backfill.

b. 32 two-dimensional elements for modeling the instrumented panels.

c. 46 joint elements for modeling the interfaces between the backfill and the walls, and between the backfill and the floor of the IRW.

d. 3 elastic springs to model the vertical and horizontal load cells.

The far field interface was assigned a very low stiffness to model the non-frictional lining applied to the far field wall. The instrumented wall elements were assigned common properties of reinforced concrete. The stiffness values of the springs used to model the horizontal load cells were determined from experimental load-deformation data of previous tests. The stiffness of the vertical load cell was calculated theoretically from the geometry and material properties of the load cells.

Table 5-7 lists property values that are representative of the structural materials in the IRW. These values were used for all the analyses. In the following section, a discussion is presented of the selection of property values for the backfill and interfaces.

Table 5-7
Summary of Property Values for Structural Materials in the IRW Analyses

Material	Property	Value
Reinforced concrete	Poisson's ratio, ν	0.2
	Unit weight, γ	23.6 kN/m^3
	Young's modulus, E	20.7 x 10^6 kPa
Spring 1	Stiffness per meter run of wall	13150 kN/m
Spring 2	Stiffness per meter run of wall	17810 kN/m
Spring 3	Stiffness per meter run of wall	24160 kN/m

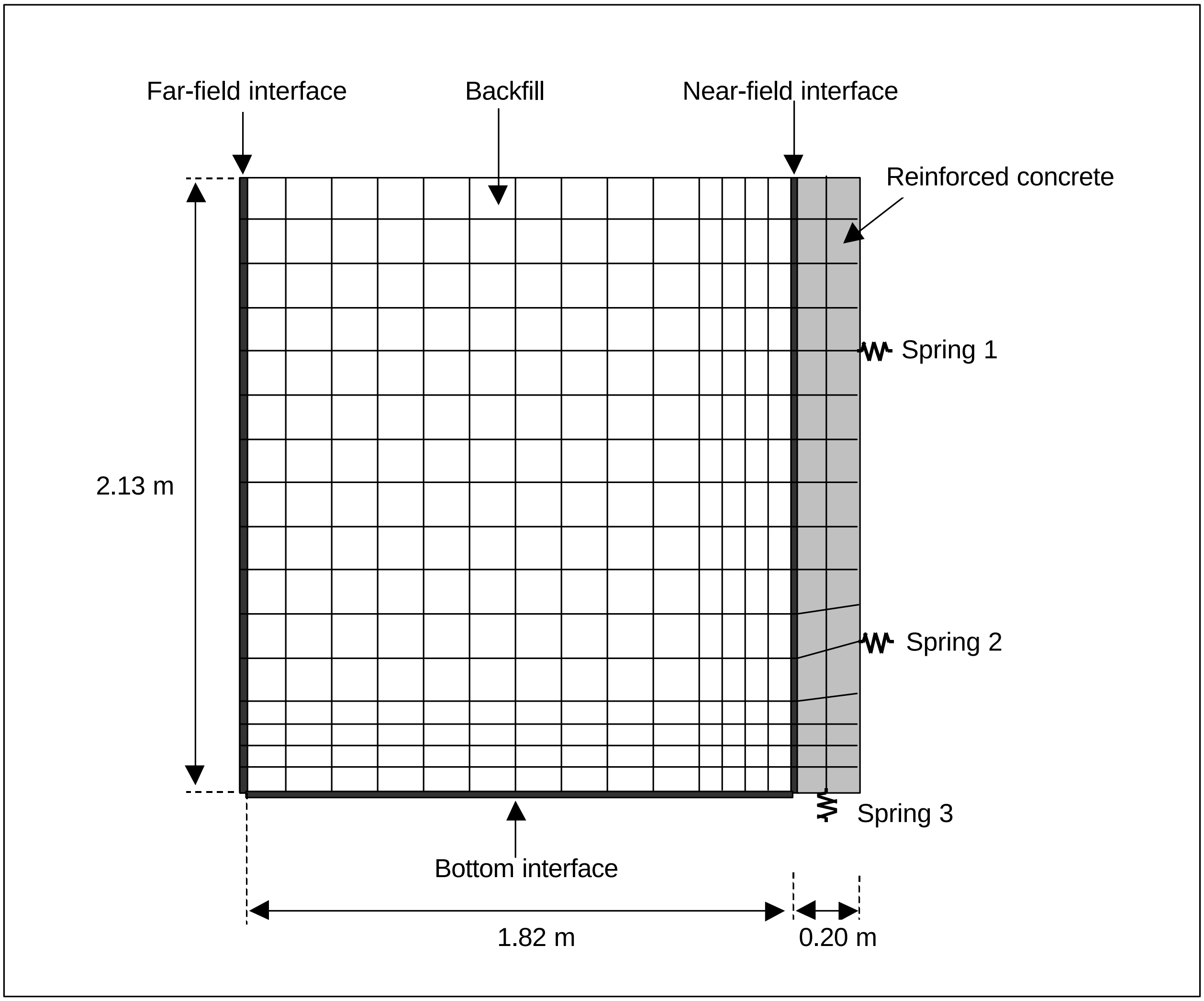

Figure 5-11. Finite element mesh used for the analyses

5.5.3 Tentative soil properties

As described in Chapter 3, hyperbolic parameter values for the Light Castle Sand were determined from triaxial and consolidation tests performed on specimens compacted to relative densities of 50 and 80 percent. A relative density of approximately 100 percent was attained during compaction of the backfill in the IRW; consequently, no direct experimental data were available on the compacted backfill properties. Tentative property values of the compacted backfill for use in the calibration analyses were determined following the procedures described in the following paragraphs.

5.5.3.1 Estimation of modulus number, *K*. Duncan et al. (1980) reported hyperbolic parameter values for a number of granular soils. They noted that there is a direct relationship between the relative density of the soil and the value of modulus number *K*. The results of the tests performed on the Density Sand and the Light Castle Sand confirm these observations, as shown in Figure 3-3. Therefore, it is possible to estimate the value of *K* by extrapolation of the values determined from the triaxial tests.

A range of tentative values of *K* determined from extrapolation is listed in Table 5-8. Both the test results and the data reported by Duncan et al. (1980) were used for this extrapolation. These values were adjusted during the analyses of backfilling and surcharge, to account for the effects of compaction on the lateral stresses in the backfill. This is discussed in the section on calibration analyses.

Table 5-8
Tentative Property Values for the Light Castle Sand Backfill

Property[1]	Tentative Value
K	800 - 1600
n	0.20
R_f	0.85
ν_{nom}	0.3 - 0.40
K_{ur}	800-1600
ϕ'	47°
γ	16.8 kN/m^3

[1] Material parameters are listed and defined in the Notation (Appendix F).

Estimation of modulus exponent *n*. According to Duncan et al. (1980), the value of *n* does not vary significantly with relative density. Therefore, the average value of *n* from the triaxial tests can be used directly. However, additional considerations need to be made for the selection of *n* in finite element analyses of the IRW.

As discussed previously, the lateral stress distribution in the compacted backfill in the IRW is not linear. Relatively large horizontal stresses exist at shallow depths inside the backfill that are induced by the stresses applied during compaction. On the other hand, finite element analyses using SOILSTRUCT-ALPHA do not model compaction effects and produce stress distributions that tend to be linear, with lateral stresses at shallow depths being relatively small.

Figure 5-12 shows the lateral earth pressures measured at the end of backfilling in the IRW. The solid line is the pressure distribution assumed for the purposes of the following discussion. For comparison, the pressure distribution obtained from a SOILSTRUCT-ALPHA analysis is also shown. Both distributions produce approximately the same magnitude of lateral force F'_x. In the upper portion of the wall, the measured lateral stresses are larger than the stresses from the finite element analyses (Figure 5-12a). Conversely, the lateral stresses from the analyses are larger than the measured stresses in the lower portion of the wall. Although no measurements were made of the lateral stresses in the backfill away from the wall, it is reasonable to assume that a similar situation occurs throughout the soil mass.

Figure 5-12b is a hypothetical diagram of an arbitrary stress-dependent property versus confining pressure. The solid line corresponds to the relationship determined from hypothetical laboratory tests. Soil properties such as the Young's modulus and the bulk modulus follow this type of relationship, as discussed in Chapter 3. The property values are inaccurate if they are determined using the solid line and the stresses from the finite element analysis. An adjusted relationship with a shallower slope, shown as a dashed line in the figure, allows estimation of approximate property values using the confining stresses from the analyses.

In order to illustrate the determination of the adjusted relationship, two points, *A* and *B*, are represented in Figure 5-12b. Point *A* is located in the upper portion of the backfill. Point *B* is located in the lower portion of the backfill. As illustrated in Figure 5-12b, the property value corresponding to the lateral stress σ^A at a point such as *A* is assigned to the lower value of stress σ_{FE}^A, calculated from the finite element analyses. Conversely, the property value corresponding to the lateral stress σ^B at a point such as *B* is assigned to the larger value of stress σ_{FE}^B, calculated from the finite element analyses. The resulting relationship has a shallower slope. If the stress-dependent property plotted in the diagram is the initial Young's modulus E_i of the soil, the slope of the relationship corresponds to the value of the modulus exponent *n*. Therefore, a lower value of *n* than that

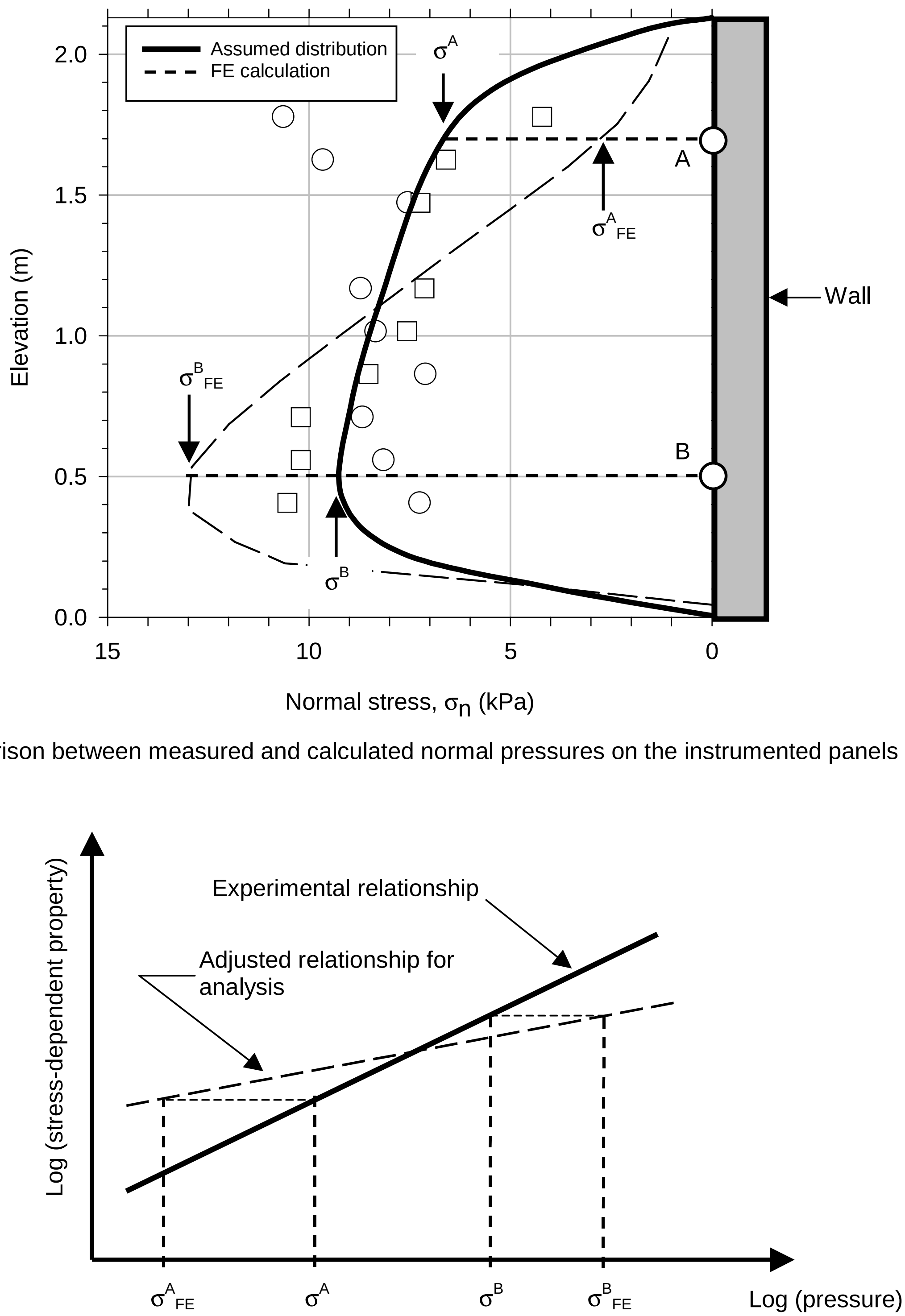

a) Comparison between measured and calculated normal pressures on the instrumented panels

b) Adjustment of stress-dependent property value

Figure 5-12. Adjustment of stress-dependent backfill property for finite element analyses of the IRW determined from the triaxial tests is required for the finite element analyses of the IRW.

Stress distributions, obtained from a series of preliminary analyses using SOILSTRUCT-ALPHA, were compared to the results of the IRW test. Based on these comparisons, an apparent value of n, listed in Table 5-8, was determined for the analyses. No further adjustments were made to the value of n during the analyses.

It must be noted that this procedure for the determination of the value of n applies only to the case of the IRW or any other walls of similar height. In lock walls, backfill heights are typically larger than 12 m (40 ft) and the lateral stresses induced by the overburden exceed the stresses induced by compaction. Consequently, adjustment of the value of n is not necessary for SOILSTRUCT-ALPHA analyses of lock walls.

5.5.3.3 Estimation of the failure ratio R_f. Duncan et al. (1980) noted that the value of R_f does not vary significantly with relative density. This was confirmed by the results of the triaxial tests performed on the Density Sand and Light Castle Sand, as observed in Table 3-3. The value of R_f assigned to the compacted backfill for the analyses is the average of the R_f values determined from the laboratory tests. No further adjustments were made to this value during the analyses.

5.5.3.4 Estimation of the nominal Poisson's ratio ν_{nom}. The value of ν_{nom} for analysis cannot be estimated directly from the results of laboratory tests. The 1-D column analysis procedure described by Ebeling and Wahl (1997) was used for a preliminary estimation of ν_{nom}. In the 1-D column procedure, finite element analyses of a column of backfill are performed. The column is free to deform in the vertical direction under the imposed loads but fully restrained in the horizontal direction. Compaction-induced stresses are not modeled in 1-D column analyses.

The 1-D column method does not provide accurate values of ν_{nom} for analyses of the IRW because significant compaction-induced lateral stresses take place in walls of low height. Additionally, vertical shear forces on the wall-backfill interface are comparatively large. A range of tentative values of ν_{nom} for analysis of the IRW is presented in Table 5-8. These values correspond to lateral loads in the 1-D column that are equal to or larger than the measured loads in the IRW. Adjustment of these tentative values of ν_{nom} was required to account for compaction effects in the IRW. For lock walls, 1-D column analyses may provide ν_{nom} values that are adequate for analysis because, due to the larger height of the lock walls, the effects of compaction on the magnitude of lateral stresses are not as significant as in the IRW.

5.5.3.5 Estimation of the unload-reload modulus K_{ur}. As discussed previously, the assumed response of the soil to unloading-reloading is linear and stress-dependent in SOILSTRUCT-ALPHA. It was assumed that a value of K_{ur} identical to the value of K may provide a reasonable approximation to the modulus value during hysteretic unload-reload cycles. The values of K and K_{ur} were adjusted simultaneously in the calibration analyses of the IRW.

5.5.3.6 Estimation of the friction angle ϕ. There is a direct relationship between the value of ϕ_o and the relative density of the soil (Duncan et al. (1980). The value of ϕ_o of the compacted backfill was estimated by extrapolation from Figure 3-3. The extrapolated value of ϕ_o and the average value of $\Delta\phi$ were used to determine the internal friction angle of the backfill according to Equation 3-1. The magnitude of the confining stress σ'_3 used for calculation of ϕ was the average of the horizontal stress measurements in the IRW test.

5.5.4 Near-field interface properties

Property values were determined for the interface between dense Light Castle Sand and concrete as described in Chapter 4. Soil specimens for interface tests were prepared with relative densities of 80 percent; therefore, no direct experimental data are available on the interface properties corresponding to the Light Castle Sand compacted to 100 percent of relative density.

There are no established criteria to predict the interface parameters based on the density of the soil. The results reported by Peterson et al. (1976) suggest that interface properties may or may not vary with relative density. In some cases, lower stiffness values were observed in dense specimens than in medium dense specimens of the same soil. In other cases, the variation in interface properties was not substantial for large changes in the soil void ratio.

Based on this information, the interface property values for the compacted backfill were assumed identical to those determined from the interface tests on the dense Light Castle Sand against concrete interface. These values, listed in Table 5-9, were used for all the analyses without further adjustments.

As discussed previously, the earth pressure distribution on the wall calculated from finite element analyses differs from the pressures measured in the IRW. For the backfill, an adjusted value of n was determined as illustrated in Figure 5-12 to account for the effect of the pressure distribution on the value of the Young's modulus. Similar analyses can be performed to determine an adjusted value of n_j that accounts for the effect of the pressure distribution on the value of interface stiffness. However, sensitivity analyses showed that n_j has negligible influence on the magnitude of the forces acting on the wall. Consequently, the value of n_j determined from the interface tests was used for the analyses.

Table 5-9
Property Values of the Wall-Backfill Interface used for the Finite Element Analyses of the IRW

Parameter [1]	Value (Determined in Chapter 4)
K_I	20700
n_j	0.79
R_{fj}	0.79
δ	33.7^{o}

[1] Material parameters are listed and defined in the Notation (Appendix F) and Appendix B.

5.6 Calibration Analyses

A series of preliminary analyses were performed for the backfilling and surcharge stages of the IRW test. The goals of these analyses were:

a. To adjust the tentative backfill parameter values determined from the laboratory tests on Light Castle Sand specimens.

b. To provide a reasonable approximation of the stresses existing in the wall-backfill system before the start of the inundation stage.

The values of horizontal and vertical forces F'_x and F_v, measured in the IRW at the end of compaction and at the end of surcharge, were the target values for the calibration analyses. The backfill property values were adjusted until the results of the analyses were approximately equal to the target values. The adjusted parameter values for the surcharge stage were used for the analysis of backfill inundation.

5.6.1 Analysis of backfilling

During the backfilling analyses, the target magnitudes of F_v and F'_x at the end of backfilling were attained by adjusting the values of modulus number K and nominal Poisson's ratio ν_{nom}. An increase in the value of K produces a decrease in vertical displacements in the backfill and, consequently, a decrease in the shear force at the wall-backfill interface. An increase in ν_{nom} produces an increase in the horizontal force magnitude. A trial-and-error process is necessary because changes in K and ν_{nom} also induce changes in F'_x and F_v, respectively.

Table 5-10 lists the property values determined from this iteration process. Figure 5-13 compares the measured and calculated values of F'_x and F_y.

Table 5-10
Backfill Property Values Determined from Calibration Analyses of Stage 1 of the IRW Test

Property[1]	Value
K	1000
n	0.20
R_f	0.85
ν_{nom}	0.36
K_{ur}	-
ϕ'	47°
γ	16.8 kN/m³

[1] Material parameters are listed and defined in the Notation (Appendix F).

The analysis showed that varying K and ν_{nom} within their expected range of values listed in Table 5-8 produces large variations in the results of the analyses. Therefore, it is not possible to make first-order predictions of backfilling in the IRW using the property values obtained from laboratory tests. However, once the target values of the forces at the end of backfilling are attained, the results of the analysis for intermediate backfill heights are in excellent agreement with the test data, as shown in Figure 5-13. This suggests that the procedures followed for the analyses are adequate, and that the models of soil and interface provide reasonable approximations to their actual response.

5.6.2 Analysis of surcharge application and removal

The analysis of the surcharge stage was performed consecutively after the backfilling analysis. Therefore, the initial forces acting on the wall before surcharge application corresponded to the values measured at the end of backfilling. The surcharge analyses were performed in two steps:

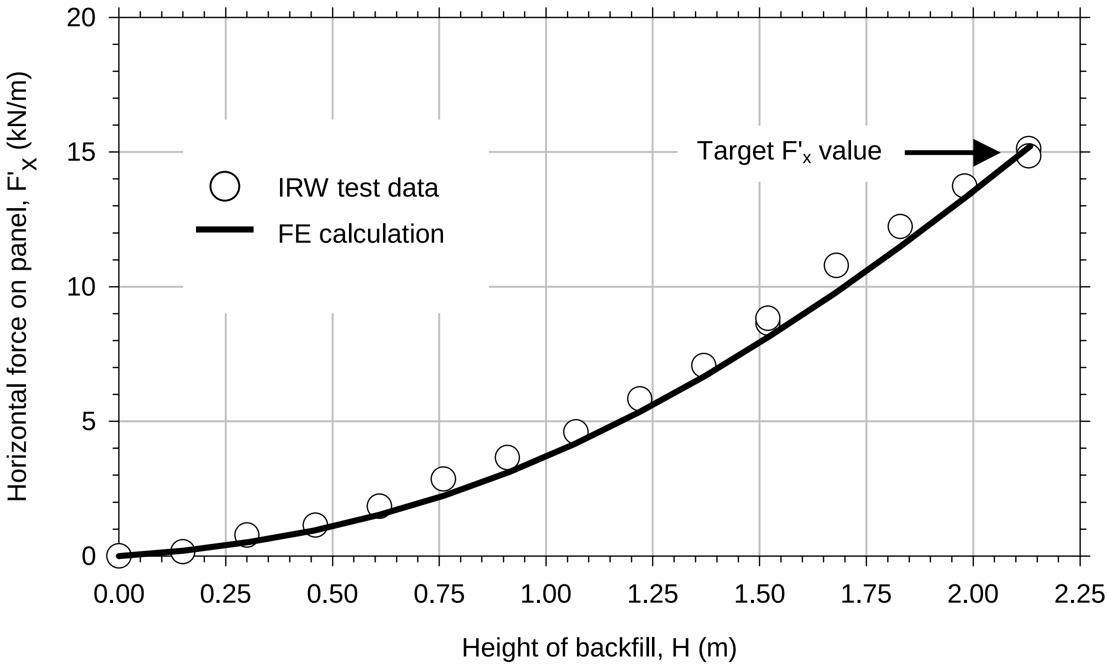

a) Horizontal forces

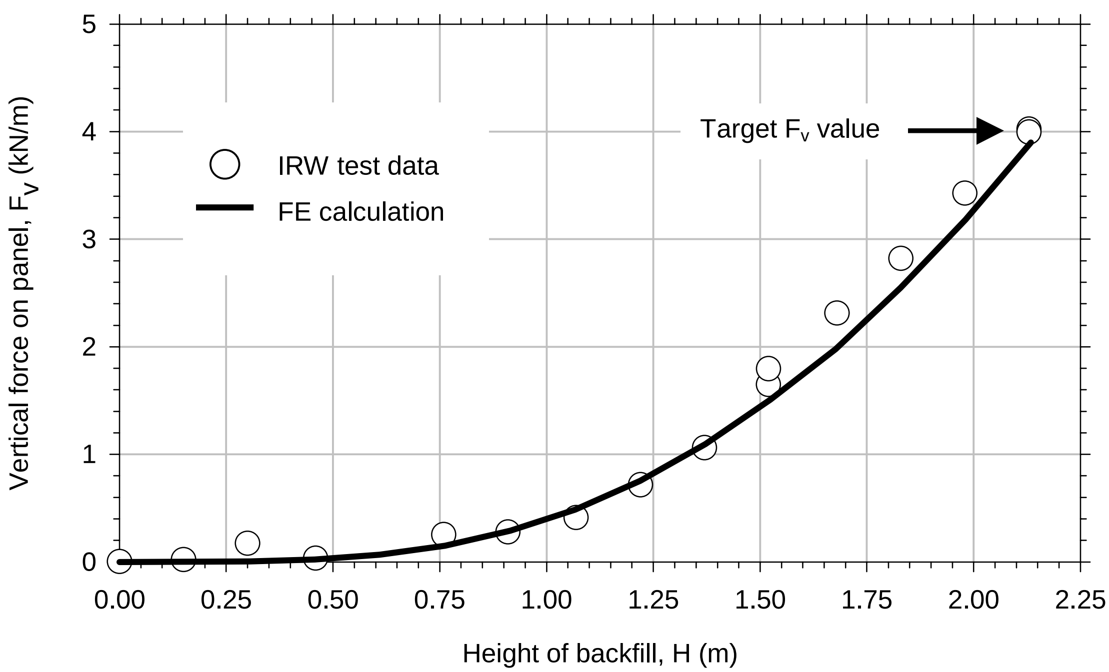

b) Vertical forces

Figure 5-13. Results of calibration analyses of backfilling and comparison to IRW test data

1. The values of K and ν_{nom} were adjusted during the analyses in order to match the target values of F_v and F'_x for full surcharge application.

2. An analysis of surcharge removal was performed using the same parameter values determined in Step 1 and assuming a value of K_{ur} identical to the value of K.

The parameter values of the backfill determined from these analyses are listed in Table 5-11. It can be observed that a larger value of K is necessary to model surcharge application than to model backfilling. Conversely, a smaller value of ν_{nom} is necessary to model surcharge application than to model backfilling. As discussed previously, the differences in the values of K and ν_{nom} between backfilling and surcharge application are due to the existence of compaction effects during backfilling that are not modeled in SOILSTRUCT-ALPHA. The values of K and ν_{nom} in Table 5-10 were selected to account for these compaction effects, and they are not representative of the properties of the compacted backfill. The soil property values listed in Table 5-11, on the other hand, are believed to be representative of the compacted backfill, and were used for the analysis of inundation described in the following section.

The value of K obtained from these analyses is larger than the expected value from the laboratory tests. This may be due to the following:

a. The laboratory specimens were prepared by pluviation, whereas the backfill was compacted by vibration. The difference in the preparation procedures may account for differences between the properties of the laboratory specimens and the compacted backfill.

b. Compaction stresses applied to each lift induce preloading of the backfill. Because the height of the IRW is relatively small, it is possible that these preloading stresses are not exceeded throughout the soil mass during subsequent application of the surcharge. Consequently, surcharge application may correspond to reloading and induce a stiffer backfill response, especially at shallow depths.

Table 5-11
Backfill Property Values Determined from Calibration Analyses of Stage 2 of the IRW Test

Property[1]	Value
K	2500
n	0.20
R_f	0.85
ν_{nom}	-0.06
K_{ur}	2500
ϕ'	47°
γ	16.8 kN/m^3

[1] Material parameters are listed and defined in the Notation (Appendix F).

The value of ν_{nom} is negative. It must be recalled that ν_{nom} does not have direct physical meaning. Considering an average stress level of the backfill of 0.23, determined from the analyses, and using Equation 5-12, an average value of the Poisson's ratio ν of 0.14 is obtained.

Figure 5-14 compares the measured and calculated values of F'_x and F_v. In the finite element analyses, the initial values of F'_x and F_v are different from the residual values after removal of the surcharge because the responses of the backfill and the interface are different during primary loading from those during unloading. Due to the scatter of the test data, it is unclear if this aspect of the analyses is representative of the actual response of the wall-backfill system.

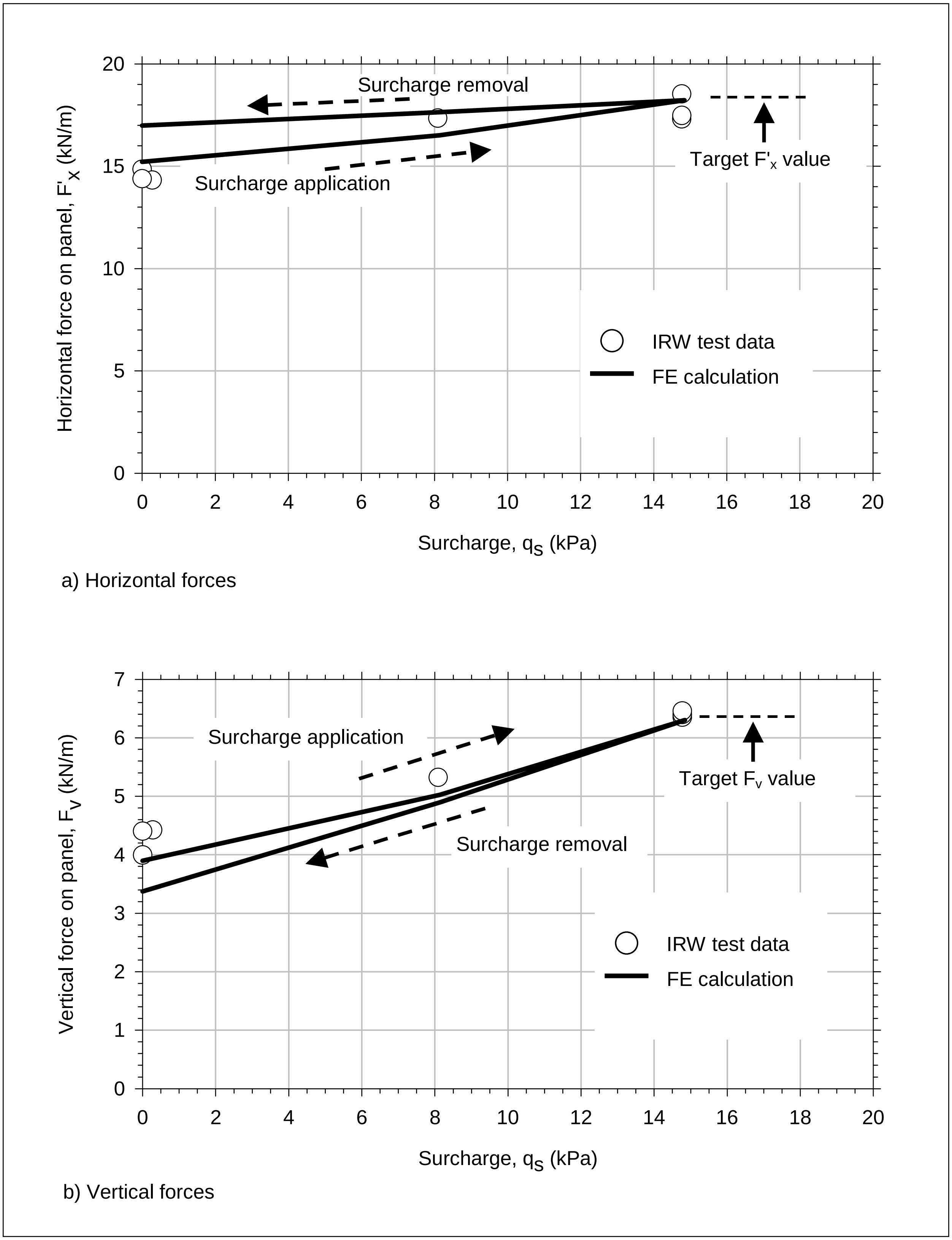

Figure 5-14. Results of calibration analyses of surcharge and comparison to IRW test data

5.7 Analysis of Backfill Inundation

An analysis was performed of the inundation stage of the IRW test consecutively after the analysis of backfilling and surcharge described in the previous section. The backfill property values listed in Table 5-11 were used for the analysis. The rise of the water level from the bottom to the top elevation of the wall was modeled in 14 incremental steps.

The results of the analyses are represented graphically in Figure 5-15 and compared to the test data. The analysis provides a very good approximation to the values of F'_x and F_v measured during the test. Three important conclusions can be made from the analysis results:

a. The implementation of the extended hyperbolic model in SOILSTRUCT-ALPHA was successful.

b. The soil and interface models used in the analyses are accurate for the type of loading that takes place during inundation of the IRW backfill.

c. It may be inferred that the interface model may be accurate for analyses of actual lock walls of greater height. Therefore, use of the interface model for lock wall analyses is recommended for further validation of its accuracy and advantages.

5.8 Summary and Conclusions

A pilot-scale test was performed in the IRW to simulate construction and operation of a lock wall. The test was carried out in three stages: backfilling, surcharge application, and backfill inundation. Light Castle Sand was used as backfill material for the test. The properties of the backfill and of the wall-backfill interface were estimated from the results of the laboratory tests described in Chapter 3.

The IRW was not originally designed for surcharge application and inundation of the backfill. Consequently, preparations were necessary to accommodate the intended simulation. In order to allow full inundation of the backfill, a wooden bulkhead was designed and constructed at the bottom of the access ramp. A sealant was applied to all the gaps existing between the instrumented panels, between the panels and the floor, and along the edges of the bulkhead to prevent significant leaks during inundation of the backfill. Two perforated PVC pipes were installed for inundation and drainage of the backfill. A soil box was prepared to contain the soil used as surcharge. Before the start of the test, all the instruments were calibrated in situ and a data acquisition system was installed in the IRW.

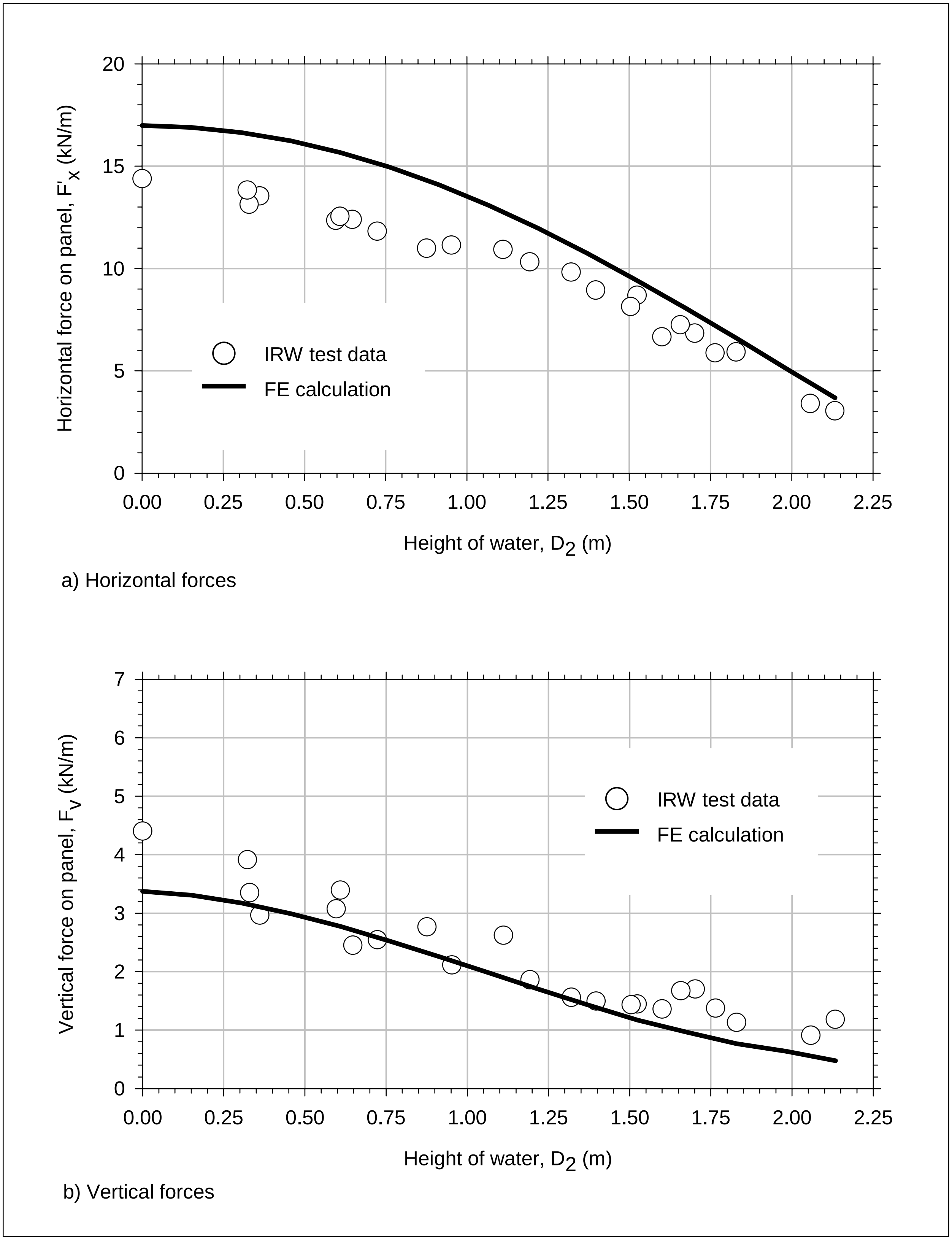

Figure 5-15. Results of finite element analyses of inundation and comparison to IRW test data

The test results show that a significant vertical shear force develops at the wall-backfill interface during placement and compaction of the backfill. This shear force increases significantly during surcharge application, and decreases during inundation of the backfill. However, it was observed that the final magnitude of the vertical shear force at the end of the test, after drainage of the backfill, was similar to the shear force at the end of backfilling. This suggests that there is no significant degradation of the vertical shear force with cycles of surcharge application and backfill inundation.

The vertical shear force coefficient K_v was calculated from the vertical force measurements during backfilling. It was found that it increases with increasing backfill height. The measured values of K_v are greater than the values predicted using the design line recommended in Appendix F of Engineer Manual 1110-2-2100 (HQUSACE, in preparation). This is a result of the conservatism employed in establishing the design line and the relatively large effect of compaction-induced stresses in short walls such as the IRW. It is not recommended here that the K_v values given by the design line be exceeded for design of lock walls.

The vertical shear force coefficient for surcharge $K_{v,q}$ was determined from the test measurements from the surcharge application stage. It was found that the design line in Appendix F of Engineer Manual 1110-2-2100 (HQUSACE, in preparation) provides a slightly conservative approximation to the measured $K_{v,q}$ value.

The correction factor C_{wt} for determining the vertical shear force coefficient during inundation was determined from the vertical force measurements during inundation and drainage of the backfill. It was found that the design line in Appendix F of Engineer Manual 1110-2-2100 (HQUSACE, in preparation) provides a good approximation of the C_{wt} value for water-to-wall height ratios D_2/H that are less than 0.5. For larger ratios, the design values are conservative.

Compaction-induced stresses are significant in the IRW because of its short height. Because the influence of compaction on the stresses decreases with increasing wall heights, accurate finite element analyses of lock walls do not commonly require modeling the stresses applied during compaction. However, for the finite element analyses of the IRW, it is important to account for these compaction effects.

The finite element analyses of the IRW were performed using the updated version of SOILSTRUCT-ALPHA, which contains the extended hyperbolic model for interfaces. For finite element analyses of the IRW, different properties were assigned to the backfill during backfilling than were assigned during surcharge application. For the backfilling analysis, a lower modulus and larger Poisson's ratio than suggested by laboratory test data were assumed, which provided appropriate vertical and horizontal stresses at the wall-backfill interface. For the surcharge placement analysis, a stiffer backfill with a reduced Poisson's ratio were assumed. The properties of the backfill were adjusted by trial and error until the analysis results matched the target values of F_v and F'_x measured in the IRW at the end of compaction and surcharge application. It was found that once a match to the target F_v and F'_x values was obtained from the analyses, the analysis results for intermediate stages also matched the test data. This suggests that the procedures followed for the analyses are adequate, and that the models of soil and interface provide reasonable approximations to their actual response.

A finite element analysis of backfill inundation was performed using the backfill properties determined from the calibration analysis of surcharge placement. The analysis provides a very good approximation to the values of F'_x and F_v measured during the test. It can be concluded that the implementation of the extended hyperbolic model in SOILSTRUCT-ALPHA was successful, and that the soil and interface models used in the analyses are accurate for inundation analyses of the IRW. It may be inferred that the model may be accurate for analyses of actual lock walls of greater height. Therefore, use of the model for lock wall analyses is recommended for further validation of its accuracy and advantages.